THE CHARACTERIZATION OF MEIOSIS-SPECIFIC COHESIN COMPONENT MUTATIONS

by

Ayobami Ward

A thesis submitted to Johns Hopkins University in conformity with the requirements for the degree of Master of Science

Baltimore, Maryland

June 2015

ABSTRACT

Cohesin is an essential structural component of chromosomes that ensures accurate chromosome segregation during mitosis and meiosis. Cohesin mutations result in a range of disorders including developmental defects, cancer and infertility, and are collectively termed "Cohesinopathies". Previous studies have shown that there are cohesin complexes specific to meiosis, required to mediate homologous chromosome pairing, recombination and segregation. The meiosis-specific cohesin complexes consist of two Structural Maintenance of Chromosomes (SMC1α/SMC1 β and SMC3) proteins, an α-kleisin protein (RAD21, RAD21L or REC8), and a stromal antigen protein (STAG3). STAG3 is a component of all meiotic cohesin complexes, interacting directly with each α-kleisin subunit. Together, these cohesins provide stability to the tripartite structure known as the Synaptonemal Complex (SC), which provides a scaffold that ensures homologous chromosomes pair and recombine during meiosis.

Our lab recently reported that germ cells from *Stag3* mutant mice arrest in early prophase ("zygotene-like" stage), due to failed homolog synapsis, impaired centromeric cohesion and defective DNA damage responses. These defects are due to meiotic cohesin instability, resulting in unstable binding to the SC. Mouse mutants for meiosis-specific α-kleisin subunits *Rad21l* and *Rec8* exhibited phenotypically distinct zygotene-like arrests that are less severe than those observed in the *Stag3* mutant. However, *Rec8*, *Rad21L* double mutants resulted in a more severe "leptotene-like" arrest accompanied by complete absence of STAG3 loading onto chromosome axes. Therefore, we hypothesized that STAG3 is required for the stability and not the initial axis loading of REC8 and RAD21L containing cohesins.

To assess interactions between STAG3 and α-kleisin subunits RAD21L and REC8, our lab has generated *Stag3*/*Rad21L* and *Stag3*/*Rec8* double knockout mice. As hypothesized, these two mutants are phenotypically distinct from one another and more severe than each single knockout mutant. *Stag3*/*Rad21L* and *Stag3*/*Rec8* double mutants exhibit further meiotic progression than the previously described *Rec8*, *Rad21L* double mutants. Our genetic analysis further demonstrates that STAG3 is necessary to stabilize meiosis-specific cohesins to the SC.

Advisor: Dr. Philip Jordan, Biochemistry and Molecular Biology

Thesis Reader: Dr. Scott Bailey, Biochemistry and Molecular Biology

ACKNOWLEDGEMENTS

I would like to acknowledge the entire Johns Hopkins Bloomberg School of Public Health, and the Jordan Lab for accepting me as an ScM student, , training me in the techniques necessary for success. I'd like to thank Jessica Hopkins and Grace Hwang for being my lab parents and making sure I looked good in the morning before going to school. Marina Pryzhkova for teaching me cell culture and giving me someone to enjoy Jazz with at work. Chantal Sottas, for my initial training, and making sure science was never boring. I would like to specially thank Dr. Philip Jordan, whose unwavering pursuit of excellence has pushed me become a better student, scientist, and man, even if he is an Arsenal fan. I would like to also acknowledge Dr. Barry Zirkin, whose commitment to young scientists is what brought me to JHSPH, and his stories form the early 20th century are what convinced me to stay.

TABLE OF CONTENTS

LIST OF TABLES

LIST OF FIGURES

INTRODUCTION

Two processes underlie the accurate reproduction of the human genome, these processes are known as mitosis and meiosis. During Synthesis-Phase (S-Phase), eukaryotic cells replicate the entirety of their nuclear DNA via semi-conservative replication [1]. These cells then enter the G-2 phase, in which the cell rapidly synthesizes proteins in preparation for division, and serves as a DNA damage checkpoint. This G_2/M checkpoint arrests the cell just before mitosis or meiosis in response to genotoxic stress as a way to assess for damaged genetic material, which is not optimal for inheritance. After crossing this checkpoint, diploid parent cells enter either mitosis or meiosis. During mitosis, sister chromatids held together by cohesin interact with the mitotic spindle, which exerts mechanical force between sister chromatids at the kinetochore attachment regions. This force allows chromatid pairs line up equidistant from the two spindle poles along the metaphase plate. Finally, in anaphase and telophase, the spindle moves the sister chromatids to opposite poles, allowing them to be segregated into two genetically identical diploid daughter cells. This process has two functions, the reproduction/growth of new cells, and the repair of damaged tissue due to the effects of stress and aging.

Meiosis, however, has a different function. Meiosis is a specialized cell division that, like mitosis, involves chromosome replication. However, after replication, meiotic cells undergo two consecutive rounds of cell division (meiosis I and meiosis II) to generate up to four haploid germ cells from the diploid parent cell (Fig.1). This reduction in ploidy is essential to sexually reproducing organisms, allowing two parent haploid gametes to fuse during fertilization, forming a zygote containing one copy of each parent's genes. Unlike in

mitosis, reductional segregation of meiosis I requires that homologous chromosomes first segregate, leaving sister chromatids to remain associated until meiosis II. During meiosis I, several important steps are taking place that ensure: 1) the proper pairing of homologous chromosomes, 2) recombination events between these chromosomes to ensure genetic diversity, and 3) proper synapsis of homologous chromosomes to avoid genetic defects, and 4) correct segregation of homologous chromosomes followed by subsequent segregation of sister chromatids during meiosis [2-3]. It is essential that these processes are highly coordinated to avoid aneuploidy and infertility. These steps generally take place within the context of meiosis I, specifically within the extended G_2 phase preceding meiosis I, known as prophase I.

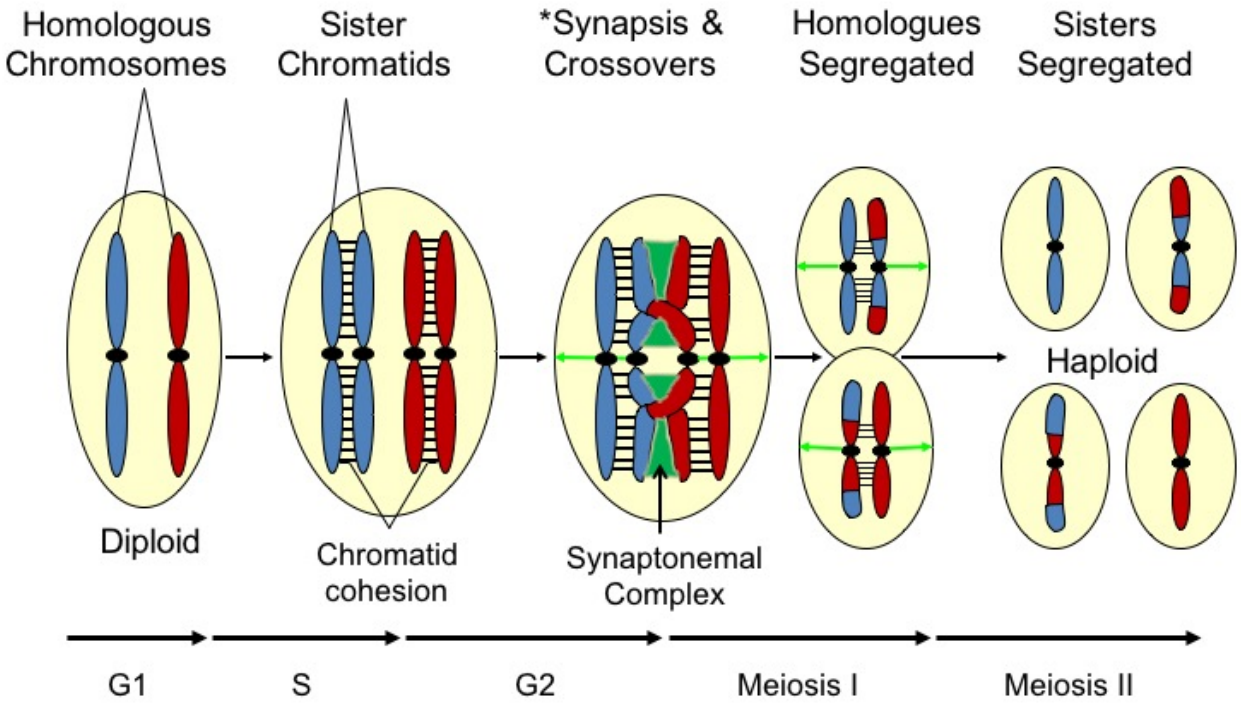

Figure 1: Illustration of chromosome dynamics in Meiosis.

Meiotic Prophase I

Prophase I is the longest phase of meiosis I, during which mechanical manipulation of chromosomes is dictated by the expression of a cadre of temporally regulated proteins. As prophase I is the period during which many of the distinctive processes in homologous recombination take place. Prophase I is segregated into 5 distinct sub-phases.: Leptonema, Zygonema, Pachynema, Diplonema, and Diakinesis (Fig. 2).

Leptonema (leptotene phase) is the first of the substages of meiotic prophase I. This term derives from the Greek words meaning *thin threads*. During this phase the duplicated chromosomes from the preceding interphase consisting of two sister chromatids condense, from diffuse chromatin structures into thin strands within the nucleus. At this point the strands begin to become visible via microscopy. However, the sister chromatids at this point are still very strongly associated with one another, and as such are virtually indistinguishable.

Zygonema (zygotene phase) is the next phase to occur during meiotic prophase I. This term derives from the Greek words for *paired threads*, and its onset is marked by the orientating of homologous chromosomes in close proximity to each other in the nuclear envelope. It is at this stage that the pairing of homologous chromosomes begins to take place, facilitated by an important proteinaceous structure known as the *synaptonemal complex* (SC). The SC facilitates the pairing events crucial to meiotic segregation and homologous recombination, and will be expanded upon at a later time. It is important to note that these chromosome pairings end at the centromere-proximal ends of the chromosomes via centromeric cohesion [4]. At this point the fully paired chromosomes are referred to as *bivalents*, indicating that each pair consists of two types of chromosomes [5].

Pachynema (pachytene phase) is the third phase in meiotic prophase I, and derives from the Greek words for *thick* threads. During this phase, the main crossover evens of homologous recombination occur. In the early stages of pachytene, synapsis between homologues is completed. During mid pachytene phase, crossover recombination events between homologous chromosomes are completed. While the autosomes undergo complete synapsis, sex chromosomes undergo a similar but not distinct process. This is due to the fact that they are mostly non-homologous, and as such only undergo a small amount of recombination at very limited area of homology known as the *pseudoautosomal regions* [6].

Diplonema (diplotene phase) is the penultimate stage in the meiotic prophase I, derived from the Greek words *two threads*. During this phase, the SC begins to degrade, allowing the homologous chromosomes to separate from each other now that recombination is complete. During this stage, the chromatin has condensed and sister chromatids in each chromosome can now be distinguished. Homologues remained paired by the crossover events visualized as chiasmata. These areas of association remain until later in anaphase I. It is here that a level of sexual dimorphism occurs in mammalian species. It is at this point in fetal oogenesis that oocytes undergo the characteristic meiotic arrest before birth, whereas male spermatogenesis, which commences during puberty, avoids this arrest and continues through meiosis. This pre-metaphase I arrest is known as dicytate.

The final stage in meiotic prophase I is known as diakinesis, from the Greek words meaning *moving through*. At this point, the chromosomes are fully condensed, and homologous chromosomes in each bivalent begin to move apart in preparation for the alignment during metaphase I. However, attachments at the chiasmata persist throughout.

As this is the final stage of prophase I, the final step is the dissolution of the nuclear envelope in preparation for the spindle fiber attachments and meiotic progression.

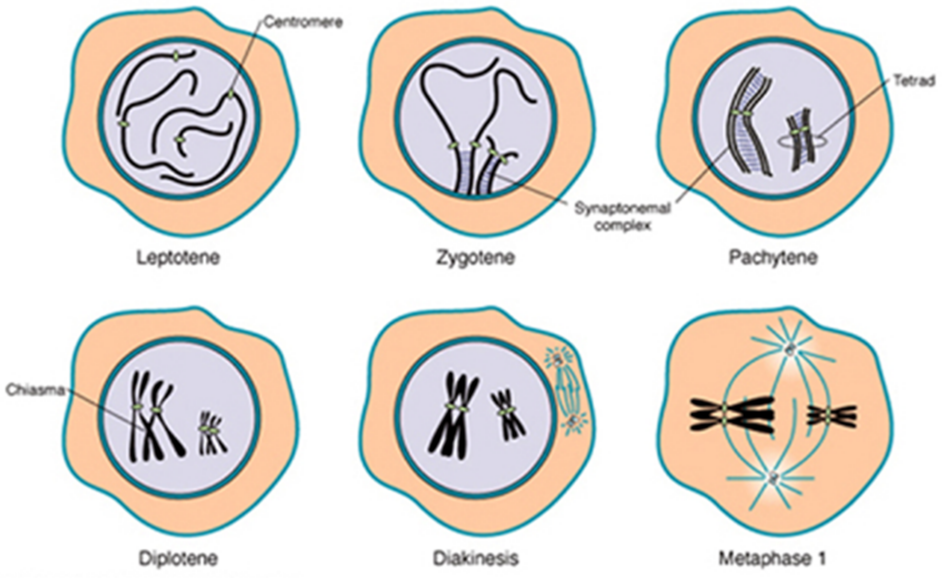

Figure 2: Illustration depicting stages of meiotic prophase I. In leptotene phase we see condensation of chromosomes, and formation of the lateral elements of the synaptonemal complex. In zygotene stage, the chromosomes approximately line up into homologous pairs. At the pachytene stage, non-sister chromatids undergo homologous recombination at specifically formed chiasmata. At diplotene stage, the SC degrades. Copyright 1999 John Wiley and Sons Inc. All rights reserved.

Homolog Pairing, Synapsis, and Recombination

Now that we have outlined the steps in meiotic prophase I, we can relate these steps to the initiation, progression, and completion of homologous recombination. Each of the first 4 phases of prophase I has an important step in the process of homologous recombination and its interplay with the synaptonemal complex, beginning with the leptotene phase. During early leptotene, the association between homologous chromosomes is facilitated by several mechanisms. During early leptotene stage, the telomeres interact with the nuclear envelope. These interactions facilitate chromosome movement. These movements are essential for initial homologous chromosome pairing [7]. However, all mouse chromosomes are telocentric, so one telomere is associated with the pericentromeric heterochromatin [8]. During leptotene stage, the pericentromeric heterochromatin of non-homologous chromosomes cluster together and form what are known as "chromoclusters" [7], [9]. These chromoclusters are important for homology search during early stages of meiosis [10-13]. The pericentromeric heterochromatin within these clusters contains repetitive DNA sequences, and the formation of chromoclusters protects these areas of nuclear attachment from the unwanted effects of recombination via suppression, allowing the proceeding attachments to occur unabated [14].

Another important mechanism by which association between sister chromatids occurs is through the presence of Synaptonemal Complex Protein 2 and 3 (SYCP2, SYCP3) [5]. These associate to form a bridge between sisters, and form what is known as the axial elements (AAs), which are essential to later progression of meiotic prophase. During this stage DNA double-strand breaks are formed by the meiosis-specific topoisomerase II-like

enzyme, SPO11 (Sporulation 11). SPO11 activity throughout the genomic DNA is the progenitor step for the initiation of a DNA-damage response-signaling cascade. SPO11 activity is required for correct meiotic progression; defects in this process can lead to infertility [15]. It is important to note that SPO11 creates double-strand breaks in non-random fashion- these occur at specific recombination hotspots in the genome [16].

Due to the presence of these breaks, the MRN complex (consisting of the Double-strand break repair proteins MRE11, RAD50, and NBS1) and the breast cancer type 1 susceptibility protein (BRCA1) associate to these sites [17]. Among their functions, one of the important purposes of these proteins is to recruit additional proteins essential to the spread of this DNA damage signal. These proteins are known as Ataxia Telangiectasia-Mutated (ATM) and Ataxia Telangiectasia Rad3-related (ATR) kinases, which phosphorylate the core histone protein H2A variant known as H2AX. Post-modification, this histone is known as γH2AX [18].

During zygotene stage, the homologous chromosomes begin to associate with their cognates to initiate homologous recombination. This coincides with homologous chromosome synapsis. At this point, the axial elements, consisting of SYCP3 and SYCP2 bridging the sister chromatids become the lateral elements (LEs) of the synaptonemal complex. At zygotene, the pairing of homologus chromosomes is facilitated by recruitment of Synaptonemal Complex Protein 1 (SYCP1) [19]. This protein forms bridges known as central region (CR) between homologous chromosomes. The action of SYCP1 can be thought of as a zipper holding the two homologous chromosomes together (Fig.3). However, SYCP1 does not act alone. Other central element proteins are known to facilitate the

SYCP1-based homologue association, known as the Synaptonemal Complex Central Element Proteins (SYCE) 1-3 an d Testis Expressed protein (TEX) 12. The presence of SYCP1-3, SYCE1-3 and TEX12 indicates the complete formation of the tripartite synaptonemal complex, consisting of two lateral elements and one central region, and allows progression through meiotic prophase I by further protein association critical to the mechanical movements required for accurate chromosome association and segregation [20].

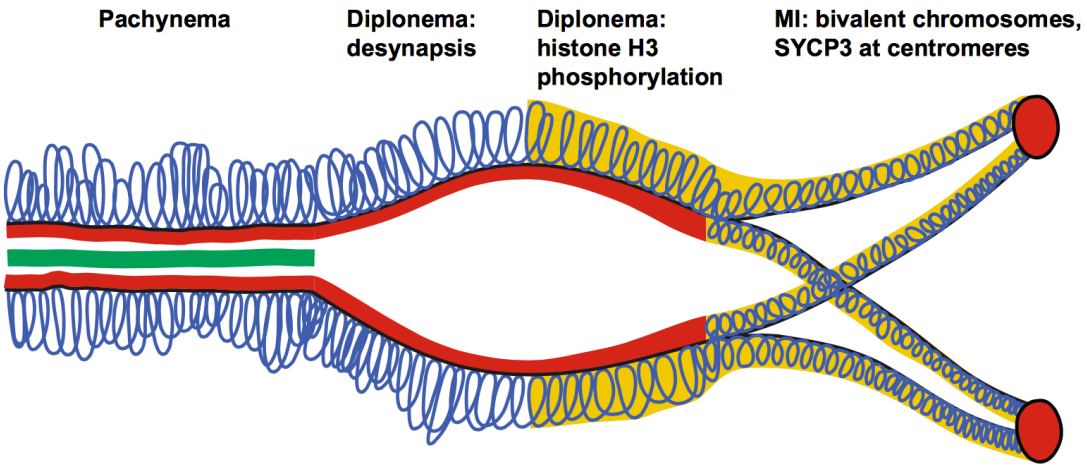

Figure 3: At the pachytene state, chromatin loops (blue) are attached to the SC LEs, marked by SYCP3 (red), and synapsis is mediated between homologues by SYCP1 (green) in the central element of the SC. Figure adapted from Sun & Handel 2008 [21].

Recombination

At this point in zygotene phase, the association between homologues allows the nucleus to begin repair of the DSBs that are present in the DNA, mainly through the recruitment of strand invasion proteins for interhomologue recombination. These two recombinase proteins of the RecA family are known as Radiation sensitive 51 (RAD51) and Disrupted Meiotic cDNA 1 (DMC1). DMC1 is meiosis specific unlike RAD51. Both promote strand exchange and forms a filament on single stranded DNA that results from SPO11 activity during leptotene. The invasion of the single strand into the unbroken homologous strand leads to the displacement of the intact strand to form a D-loop, which results in the formation of asymmetric heteroduplex DNA. At this point, there are two options by which the D-Loop may progress to be resolved: Synthesis-dependent strand annealing (SDSA) or the formation of a double Holliday Junction.

In the double Holliday Junction model, having now found a partner, DNA polymerase can now extend the 3' end of the invading DNA strand, and leads to the formation of a double Holliday junction. Homologous recombination is not a sure fire way to introduce genetic variety, as two events can take place as a direct result of the formation and resolution of the double Holliday junction – non-crossover and crossover events (Fig.4). These can result from the multiple mechanisms used to resolve the double Holliday junction. However, homologous recombination via this pathway only takes place at a subset of DSBs. In the vast majority of recombination events, the nucleus takes advantage of the SDSA model of non-crossover recombination. In this process, directly after the D-loop is formed, the action of the several DNA helicases prevents the formation of the double Holliday

junction. These proteins are known to have *anti-recombinase* activity. In yeast, this protein is known as DNA helicase Suppressor of Rad Six 2 (SRS2), and was recently discovered to have a mammalian homologue known as PCNA Associated Recombination Factor (PARI) [22-23]. Several other mamallian helicases exist that have preserved anti-recombinase function, including RecQ Protein-like 5 (RECQL5), Bloom syndrome, RecQ helicase-like (BLM) and Fanconi anemia, complementation group J (FANCJ) [24-26]. These proteins each act to inhibit RAD51 induced strand exchange leading to the formation of double Holliday junction, forcing repair via SDSA. The invasion strand is acted upon by DNA polymerase in the 5'-3' direction causing the D-loop to translocate positioning. This process is known as bubble migration DNA synthesis. As a result, we see the formation of a single Holliday junction undergoes branch migration, and leading to the formation of a 3' overhang, which can associate with the opposite end of the original break. The gaps left over in the sequence from the process are filled, and the nicks in the new sequence ligated to form recombination events independent of the double Holliday junction.

During the pachytene phase many of the crossover and non-crossover events have been repaired by recombination. Synapsis between homologues is now complete. The temporal relation between SC formation and homologous recombination is no coincidence, there is clear evidence of an interdependency between the two. Although the full gambit of interactions between the recombination machinery and the SC are unknown, recent evidence has indicated that there is an interaction between RAD51 and SYCP1, as well as with SYCE2 [27-28]. Although many of the recombination nodules have been repaired by the beginning of pachytene phase, late recombination nodules have been shown to persist through zygotene and into pachytene phase. By diplotene/diakinesis, homologues are fully condensed, and the SC dissembles.

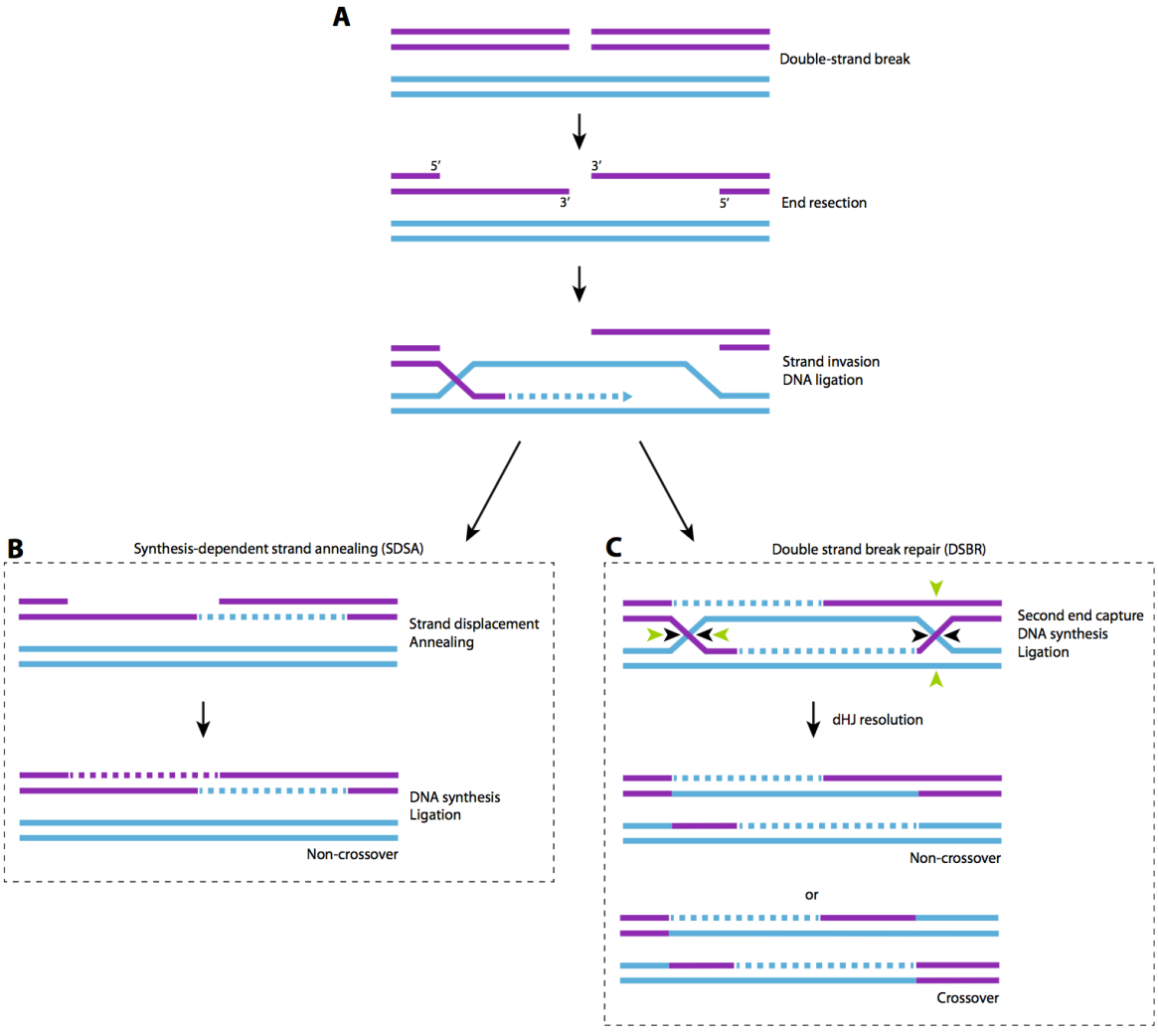

Figure 4: DNA double strand break repair by homologous recombination via Synthesis-Dependent Strand Annealing (SDSA) and Double Strand Break Repair (DSBR). Figure adapted from Verver et al. 2015 [29].

Cohesin Complex and Meiotic Prophase I

It is true that the synaptonemal complex acts as a necessary and essential scaffold upon which the events of homologous recombination may occur. However, it is just that, a scaffold. The true player directing chromosome dynamics during meiotic prophase I is known as cohesin, a protein complex component of the SC. During mitosis, its function is to hold sister chromatids together for their segregation at the metaphase to anaphase transition. However, in meiosis cohesin has a hand in all of the functions we previously outlined, from pairing at the beginning of prophase I to segregation events that take place in anaphase.

The cohesin complex consists of several individual interconnected protein subunits. The complex is made up of two structural maintenance of chromosome (SMC) proteins, heterodimerically bonded at their hinge domains. At the opposite ends, these structures are bridged by an α-kleisin protein, which is finally capped by a stromal antigen (STAG) protein. The remaining subunits show different levels of expression during mitosis and meiosis. Previous interaction studies have shown that there is one SMC1 protein (SMC1β), two α-kleisins (RAD21L and REC8) and one STAG protein (STAG3) that are meiosis-specific. Considering the different cohesin subunits and interaction studies, there are at least five meiosis-specific forms of cohesin, which together with the mitotic cohesin complex, are lateral components of the SC. Interestingly enough, STAG3 is the only meiosis-specific subunit that is represented within all meiosis-specific cohesin complexes identified [6]. The currently known forms of the cohesin complex can be seen below (Fig. 5).

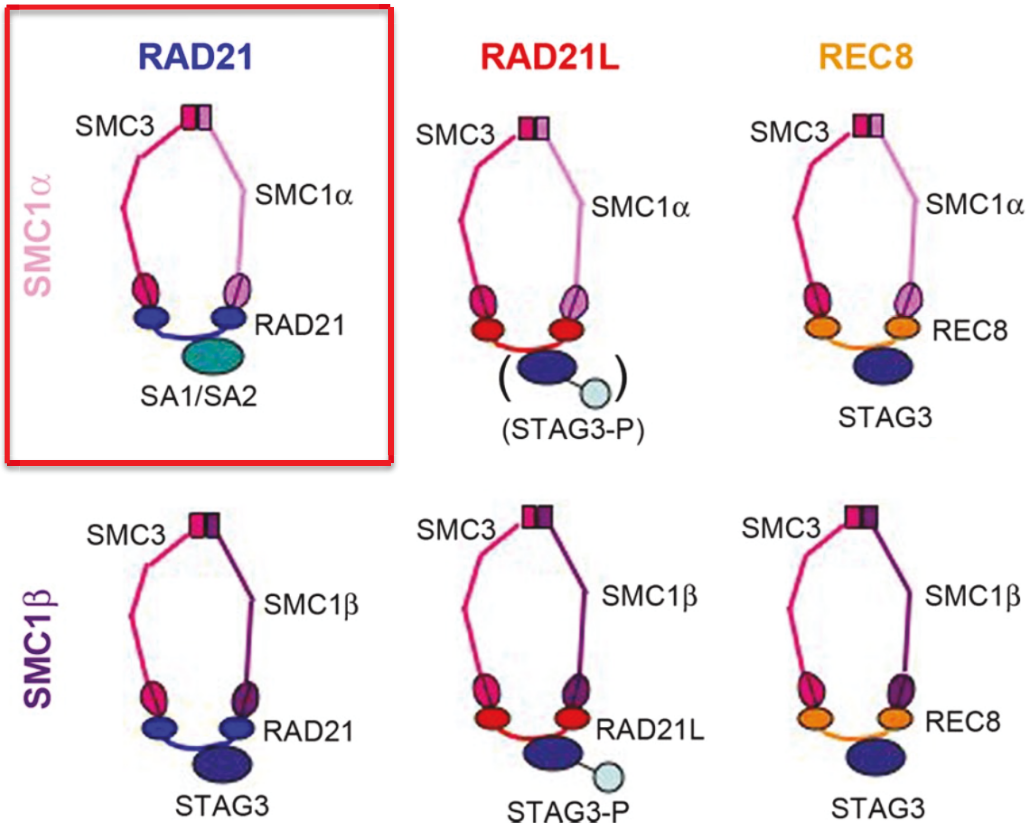

Figure 5: Putative subunit compositions of the cohesin complexes as revealed by Hirano and Lee [30]. The mitosis specific cohesin component is boxed in red. The remaining cohesin components can all be found within meiotic cells.

As we can see (Fig.5*)*, there is differential expression of the cohesin complex subunits between mitosis and meiosis. Given the structural differences, it is natural to hypothesize that cohesin has different functions in mitosis and meiosis. All cohesin complexes contain a single SMC3, and a single SMC1 (α or β) forming a heterodimer [31]. All SMC subunits are self folded by antiparallel coiled-coil interactions. This results in a distinct morphology: a rod-shaped molecule with an ATP-binding cassette (ABC)-like "head domain" where the N and C termini are juxtaposed at one end, and a hinge domain at the other [32]. While the hinge domain associates tightly independent of ATP, the ATP dependent binding of the SMC head domains drives the formation of an open V-shaped dimer (Fig.6*)*. In the cohesin complex, this structure is closed by the association between the N- and C-terminal domains of the α-kleisins (RAD21, RAD21L, REC8) to the head domains of SMC3/1 [33-35]. This allows for the characteristic closed cohesin "ring" structure.

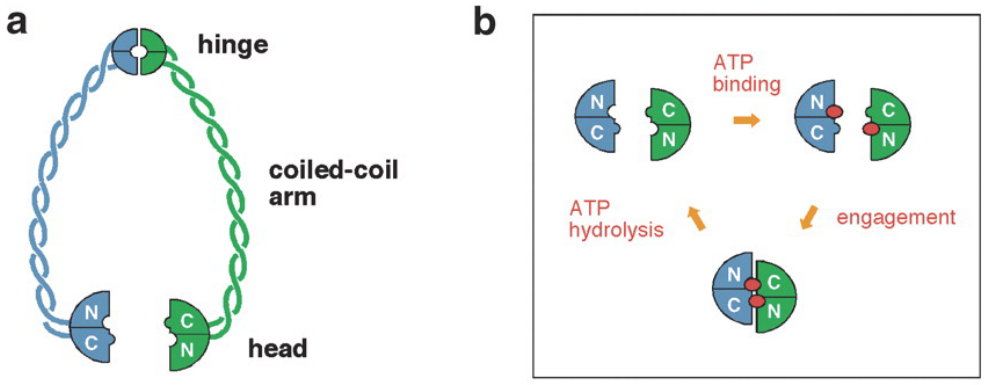

Figure 6: Model depicting the architecture of the SMC protein association. (a) The two hinges of the heterodimer interact between the two subunits, producing the ring-like structure of the cohesin complex. (b) Two units of ATP are used to catalyze the bond, and hydrolysis of these units leads to dissociation of the complex. Figure adapted from Losada & Hirano 2005 [31].

The α-kleisin proteins include RAD21, RAD21L, and REC8. These proteins define the functions of the cohesin complex during prophase I. RAD21 is expressed during mitosis and meiosis, while REC8 and RAD21L are expressed exclusively in meiosis [36]. During the pre-leptotene stage of meiotic prophase I, the different cohesin complex proteins begin to aggregate at the sister chromatid axes. Each acts as part of the larger cohesin complex [6]. However, cohesin complexes consisting of different α-kleisin proteins serve different functions in meiosis, as summarized (Fig.7). The protein REC8 is required for sister chromatid cohesion at the arms near the telomere, and cohesion at the centromere [30]. This protein has also been implicated as one of the first cohesin proteins to aggregate, showing up shortly after pre-meiotic S-phase [37]. Due to this role in preserving cohesion at the centromere, REC8 generally co-localizes at these areas well past prophase I, and into metaphase I at which point spindle interactions can allow for adequate segregation of homologous chromosomes [38]. Biochemical analyses have indicated that this is facilitated by the cleavage of REC8 by the protein separase [39]. Mutation of *Rec8* in mice causes incorrect synapsis between sister chromatids and subsequent meiotic arrest and apoptosis [34].

RAD21L, another meiosis specific α-kleisin cohesin component, has been shown to aggregate in the pre-meiotic S-phase as well. This protein can also substitute for RAD21 in the meiosis specific cohesin complex. Prior studies indicated a mutually exclusive presence of the RAD21L and RAD21 proteins during meiosis [30]. Unlike REC8, however, RAD21L has been shown to dissociate from the SC at mid pachytene stage, although the detectability of RAD21L during and past mid-pachytene has not been consistently reported [10], [30],

[35-37]. It is hypothesized that RAD21L has a function in the initiation of synapsis between homologues, such that it is required to see the homologues through to the beginning of the recombination events, but not afterwards leading to the observation that it begins to dissociate in mid-pachytene [30]. Furthermore, it has been shown that RAD21L is implicated in early telomere attachment. Mutants for the *Rad21L* gene have shown dysfunction in telomere localization, similar to that seen in *Smc1b* mutants [38]. Male mutants for RAD21L have been shown to have a morphologically different zygotene-like arrest than other mutants, exhibiting incomplete synapsis between homologues, a degree of synapsis between non-homologues and the absence of crossovers [36]. Unlike REC8, however, RAD21L is not implicated in centromere cohesion, and mutants of *RAD21L* show little defect in centromere-kinetochore localization or stability [36].

RAD21, is the final α-kleisin cohesin subunit. Unlike the other subunits REC8 and RAD21L, RAD21 is present in both mitotic and meiotic cells. RAD21, in mitosis, generally associates with the cohesin complex via interactions with STAG1 and STAG2 proteins, which are mitosis specific forms of the stromal antigen protein STAG3. RAD21 functions to facilitate synaptonemal complex stability, and some studies have implicated mutations in preventing DNA repair in certain tissues [39]. Furthermore, RAD21 seems to act in a complementary fashion to both RAD21L and REC8 in meiosis, given that the three cohesin complexes do not localize to the same areas [40].

The stromal antigen proteins are the final components of the cohesin protein complexes. The association between the cohesin complex and the STAG proteins is facilitated by an interaction with the α-kleisin subunits. There exist three STAG variants in vertebrates, STAG1-3. STAG1 and STAG2 appear only in mitotic cohesin complexes, while

STAG3 is the only STAG protein present in any of the meiosis-specific cohesin complexes [6], [41]. STAG proteins serve several functions. Recent studies have indicated that STAG1 is necessary for proper sister chromatid cohesion and telomere cohesion [42]. STAG2 has been previously been characterized as an important regulator of centromeric cohesion during replication, and depletion of STAG2 leads to loss of centromere cohesion [42-43]. STAG2 has been shown to localize in pre-leptotene and diplotene stage spermatocytes, where the STAG2/RAD21/SMC1A/SMC3 complex is thought to participate in chromatid cohesion, supporting the actions of meiotic cohesin complexes [44]. Recent interaction studies have shown that STAG3's presence in prophase I is essential to maintaining the meiosis specific cohesin complex [6]. As prophase continues, STAG3 dissociates, coinciding with the gradual removal of cohesin from the chromosome arms (staying associated at the pericentromeric regions). This residual cohesin is important for the continuation of mitosis/meiosis, and stays associated via the protection of the protein shugoshin (SGO1), until the metaphase to anaphase transition [45-47].

As previously stated, REC8 must be cleaved from the centromeric regions for meiotic progression (anaphase I). This cleavage is facilitated by the protease separase, which acts to degrade REC8 from centromeres [37], [48]. While SGO1 has been shown to protect REC8 from phosphorylation, previous work has shown that SA2 must be phosphorylated by the activity of Polo-Like Kinase 1 (PLK1) in order to allow separase to cleave the the α-kleisin subunit, specifically removing the cohesin ring from the chromosome arms [49-51]. It is possible that STAG3 serves a similar function during meiotic prophase, protecting the meiosis specific α-kleisin subunit from the action of separase until the proper time.

STAG3 requirement for Cohesin Stability

Literature examining the meiotic differences between the α-kleisin mutants *Rad21l* and *Rec8* has given us two distinct phenotypes for cohesin complex mutations. The *Rad21l* mutants, arrest at a zygotene-like stage indicated by the incomplete synapsis of homologous chromosomes in the prophase spermatocytes. The *Rad21l* mutants also show defects in repair of SPO11-induced DSB's, indicating that RAD21L containing cohesins are have an important role in homologous recombination. Furthermore, *Rad21l* mutants exhibit aberrant synapsis between non-homologous chromosomes. Mouse *Rec8* mutants, also have defects in DSB repair, as well as a zygotene-like arrest characterized by abnormal sister chromatid synapsis, which is distinct from the one reported for *Rad21l* mutants. *Rec8* mutants also suffered from impaired centromere cohesion. Given the difference in these phenotypes, it is evident that RAD21L and REC8 containing cohesin complexes have specialized functions in meiosis.

STAG3 interacts with all three α-kleisins during meiosis, and we propose that its function is to protect the α-kleisin proteins, and thus the cohesin complex from degradation Previous work from our lab supports the hypothesis that STAG3 facilitates the stability of the meiosis specific cohesin complexes. Using two independent null mutations for *Stag3*, known as the JAX allele and the OV allele, our lab showed that the absence of STAG3 resulted in a more severe zygotene-like arrest than the *Rec8* or *Rad21l* mutants, but shared common defects with both. In summary, the *Stag3* mutant displayed defective axial element formation, synapsis between sister chromatids, an inability to repair SPO11-induced DSBs and reduced retention of centromeric cohesion (Fig.7) [6]. In addition, components of the

meiosis-specific cohesin complexes were destabilized, supporting the hypothesized role of STAG3.

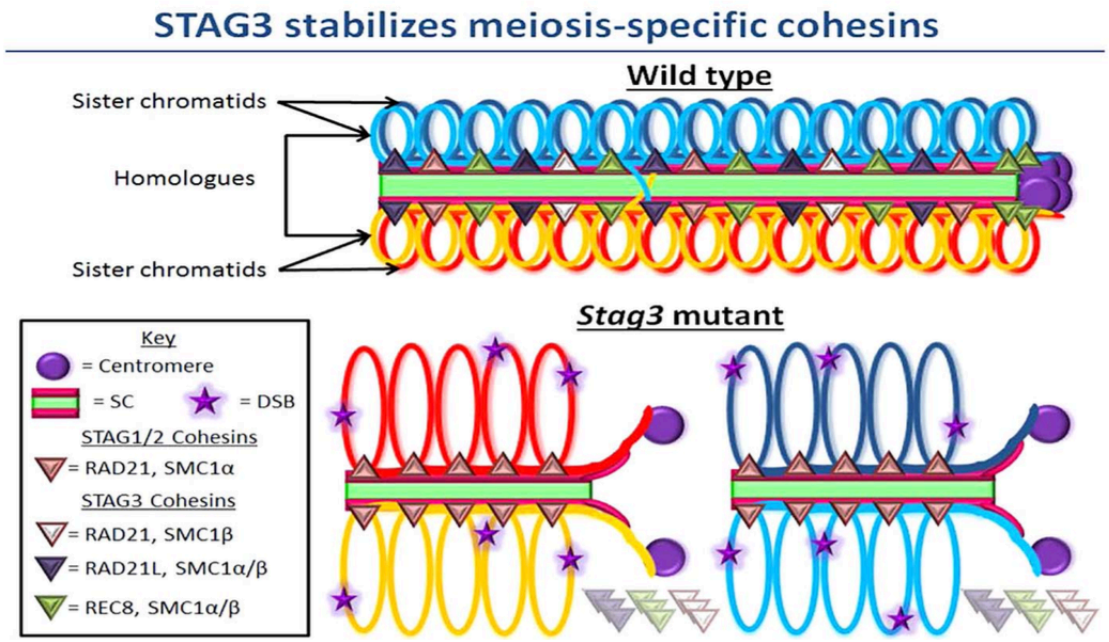

Figure 7: Illustration depicting a pachytene stage wild-type vs. a zygotene-like Stag3 mutant. During the pachytene stage, homologues are fully synapsed and the crossovers have already taken place. However, in the Stag3 mutant, localization and stability of the meiosis-specific cohesin complexes leads to synapsis between sister chromatids. Furthermore, we see unrepaired DNA double-strand breaks, and defective centromere cohesion. Figure from Hopkins et al 2014 [6].

Current Project and Hypothesis

Using phenotypic endpoints such as meiotic progression, chromosome synapsis, DNA damage repair, centromere cohesion, and localization of meiosis specific cohesin proteins, our lab's study of the *Stag3* mutant have led to a valuable hypothesis: STAG3 is required for the stable localization of the meiosis specific cohesin components onto chromosome axes in meiotic prophase I. As previously stated, mutation of each meiosis-specific α-kleisin has been shown to cause different forms of meiotic prophase arrest in spermatocytes. *Rad21l* mutation results in zygotene-like arrest, non-homologous synapsis, partial aggregation of the CE (SYCP1), and unrepaired DSBs. R*ec8* mutation produces zygotene like arrest, centromere cohesion defects, unrepaired DSBs, and synapsis between sister chromatids. Mutation in *Stag3* results in a similar zygotene-like arrest to the *Rec8* mutant, although it is more severe (shorter axes). The double mutant *Rad21l/Rec8* showed a leptotene-like arrest, and almost non-existent levels of SYCP1 localization. Furthermore, researchers observed a much lower number of axes, coupled with more SYCP3 aggregates indicating that somehow REC8 and RAD21L are necessary for the formation of AEs and LEs.

If STAG3 really is a necessary component of all meiosis-specific cohesin complexes, then it is interesting that the phenotype is less severe than that of the *Rad21l/Rec8* double mutant [52]. As shown in Figure 5, the SMC1/SMC3 heterodimer is connected by RAD21L, RAD21, or REC8. The STAG protein "caps" the α-kleisin forming a full cohesin complex. According to this model, STAG3 might not be required for cohesin ring formation, but for stability of the cohesin ring itself. Previous data supports this argument, as there are lower levels of SMC1B, REC8, and RAD21L on the axes in the *Stag3* mutant. To further test this

hypothesis, and to determine why we observe a less severe phenotype in the *Stag3* mutant than the *Rad21l/Rec8* mutant we generated *Stag3/Rec8* and *Stag3/Rad21l* double mutants. We hypothesize that these phenotypes will be less severe than the *Rad21l/Rec8* with respect to axial element formation, since the option to use the reciprocal STAG3 containing cohesin still exists. However, the *Stag3/Rec8* and *Stag3/Rad21l* mutants have not been generated or analyzed. If STAG3 is indeed required for the *stability* of meiosis-specific cohesin complexes in meiosis, compared to the *Stag3* single mutant, we should see a more severe phenotype in the *Stag3/Rad21l* and *Stag3/Rec8* double mutants but still less severe than the *Rad21l/Rec8* which has no reciprocal cohesin alternative.

In order to further assess the phenotypic changes in spermatocytes co-mutated for *Stag3* and *Rad21l* or *Rec8*, we have generated three independent null mutations for *Rad21l*, *Rec8*, and *Stag3*. Furthermore, we have generated three novel null mutations for the *Stag3/Rad21l*, *Stag3/Rec8*, and *Rad21l/Rec8* genotypes. We expect the *Stag3/Rad21l* and*Stag3/Rec8* double mutant mice to exhibit a more pronounced meiotic defects than the single mutants, namely an increased number of unsynapsed axes, more severe DNA damage responses, and centromere cohesion defects. However, these double mutations should not be equivalent (Fig.8). We also expect that these double knockout mutations will, themselves, be less severe than the phenotype presented in the *Rad21l/Rec8* genotype. These proposed observations would support our hypothesis that STAG3 is required for the stability of meiosis-specific cohesins, but not the ability to associate with the chromosome axes during meiosis.

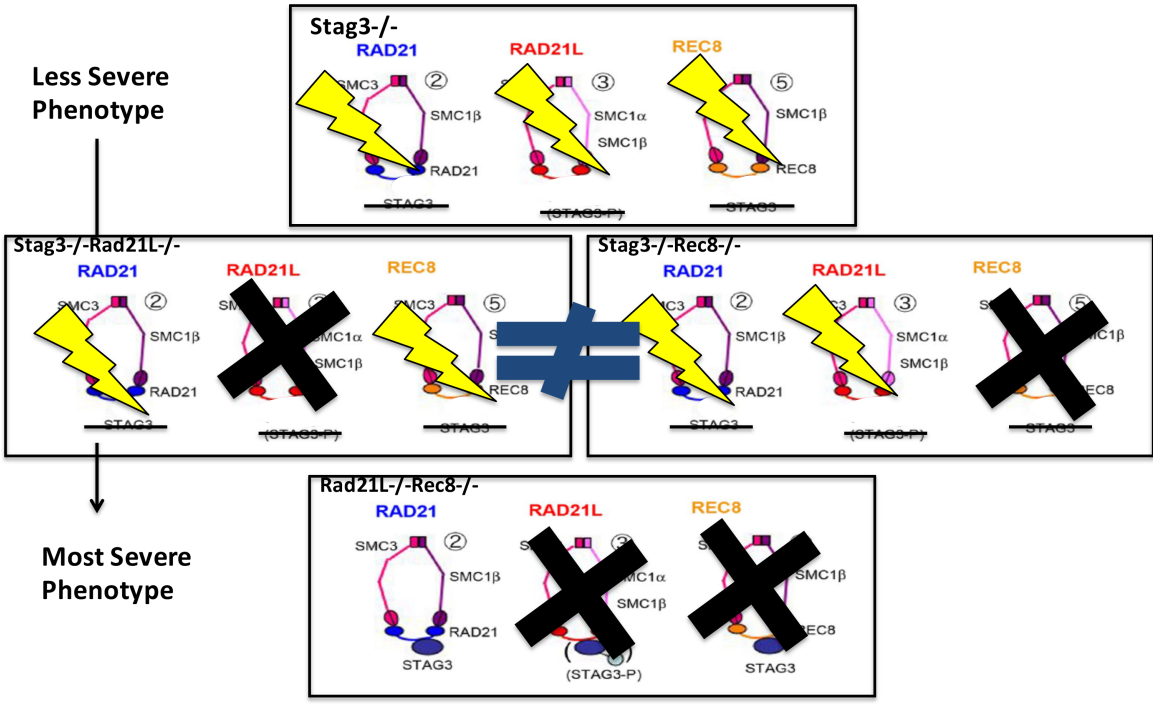

Figure 8: Model depicting the expected distribution of phenotypes among mutations for Stag3

Intended to be blank

MATERIALS & METHODS

Ethics statement

All mice were bred by the investigators at The Jackson Laboratory (JAX, Bar Harbor, ME) and Johns Hopkins University (JHU, Baltimore, MD) under standard conditions in accordance with the National Institutes of Health and U.S. Department of Agriculture criteria and protocols for their care and use were approved by the Institutional Animal Care and Use Committee (IACUC) of The Jackson Laboratory and Johns Hopkins University.

Stag3 OV and *Stag3 JAX* Mice

Two mutations for *Stag3* were used in this study. 1–8 cell stage FVB/N embryos were mutated by random insertion of the SB-cHS4core-SB-Tyro-WPRE-FUGW lentiposon transgene (LV2229). Using inverse PCR analysis, the lentiviral integration site was identified in intron 8 of the stromal antigen 3 gene (*Stag3*) on chromosome 5. The 3'-LTR is linked to the (+) strand of DNA at position 138,735,815 bp [NCB137/mm9; 3'-138,735,815(+)]. The lentivirus is inserted in the sense orientation relative to the disrupted mouse gene (Fig.9A, http://www.mmrrc.org/catalog/sds.php?mmr rc_id=36275). The resulting heterozygote mice (FVB/N-*Stag3*$^{TgTn(sb\text{-}cHS4,Tyr)2312COve}$/Mmjax) were bred together to create homozygote offspring which were compared to heterozygote and wild type littermate controls. These mice were referred to as the *Stag3 OV* line. Next, C57BL/6N-derived JM8.N4 embryonic stem (ES) cells that were targeted with a *β-galactosidase* containing cassette that generated a knockout first reporter allele for *Stag3* that harbored a floxed exon 5 were sourced from the International Knockout Mouse Consortium [53], http://www.knockoutmouse.org/martsearch/ project/22907). As part of the KOMP2

program (http://commonfund.nih.gov/KOMP2/) these ES cells were injected into B6(Cg)-Tyrc-2J/J blastocysts. The resulting chimeric males were bred to C57BL/6NJ females and then to B6N.Cg-Tg(Sox2-cre)1Amc/J mice to remove the floxed neomycin and exon 5 (Fig.9B). Offspring were bred to C57BL/6NJ mice or to wildtype siblings to remove the cre-expressing transgene resulting in the heterozygote B6N(Cg)-Stag3$^{tm1b(KOMP)Wtsi}$/2J strain used in this study. Offspring homozygous for the Stag3$^{tm1b(KOMP)Wtsi}$/2J allele were compared to heterozygote and wild type littermate controls.

Rec8 Mutation

The *Rec8* mutant mice used in our study has previously been described (Fig.10A) [37].

Rad21l Mutation

The *Rad21l* mutant mice used in our study was generated as follows. C57BL/6N-derived JM8.N4 embryonic stem (ES) cells that were targeted with a *β-galactosidase* containing cassette that generated a knockout first reporter allele for *Rad21l* that harbored a floxed exon 3 were sourced from the International Knockout Mouse Consortium [53], http://www.knockoutmouse.org/martsearch/ project/22907). As part of the KOMP2 program (http://commonfund.nih.gov/KOMP2/) these ES cells were injected into B6(Cg)-*Tyr^{c-2J}*/J blastocysts. The resulting chimeric males were bred to C57BL/6NJ females and then to B6N.Cg-Tg(Sox2-cre)1Amc/J mice to remove the floxed neomycin and critical exon sequences (Fig.10B). Offspring were bred to C57BL/6NJ mice or to wildtype siblings to remove the cre-expressing transgene resulting in the heterozygote B6N(Cg)-*Rad21l$^{tm1b(KOMP)Wtsi}$*/J strain used in this study. Offspring homozygous for the *Rad21l$^{tm1b(KOMP)Wtsi}$*/J allele were compared to heterozygote and wild type littermate controls.

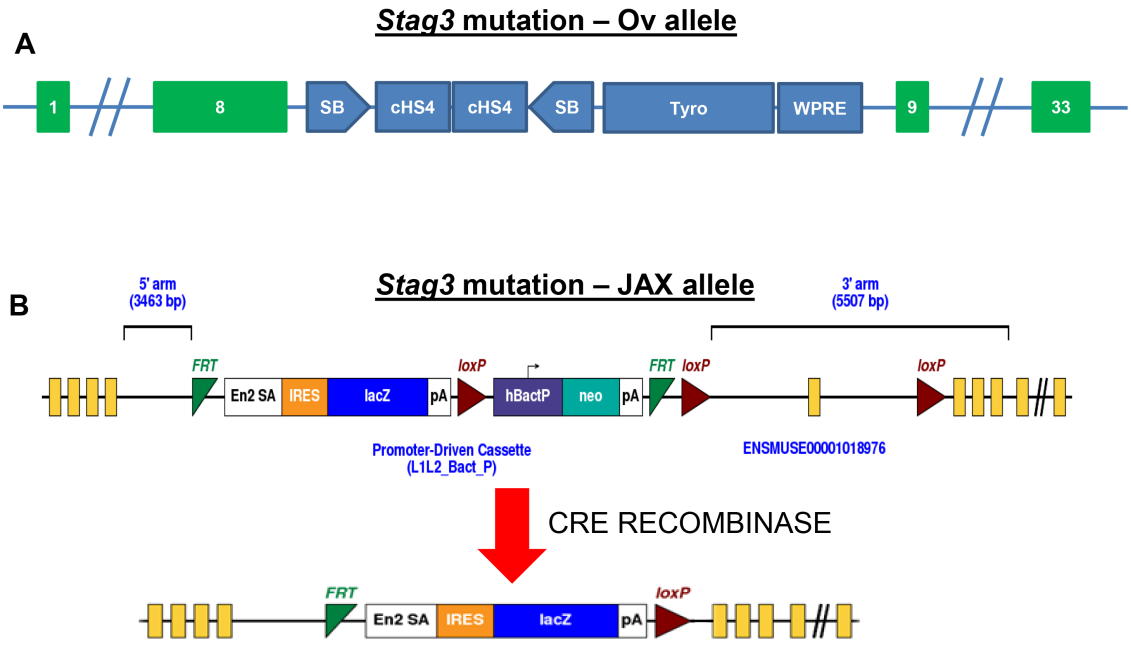

Figure 9: Two Stag3 mutants used for this study. (A) Stag3^{Ov} mutant allele: 1-8 cell stage FVB/N embryos were mutated by random insertion of the SB-cHS4core-SB-Tyro-WPRE-FUGW lentiposon transgene (LV2229) (B) Stag3^{JAX} mutant allele: C57BL/6N-derived JM8.N4 embryonic stem (ES) cells that were targeted with a β-galactosidase containing cassette that generated a knockout first reporter allele for Stag3 that harbored a floxed exon 5 were sourced from the International Knockout Mouse Consortium.

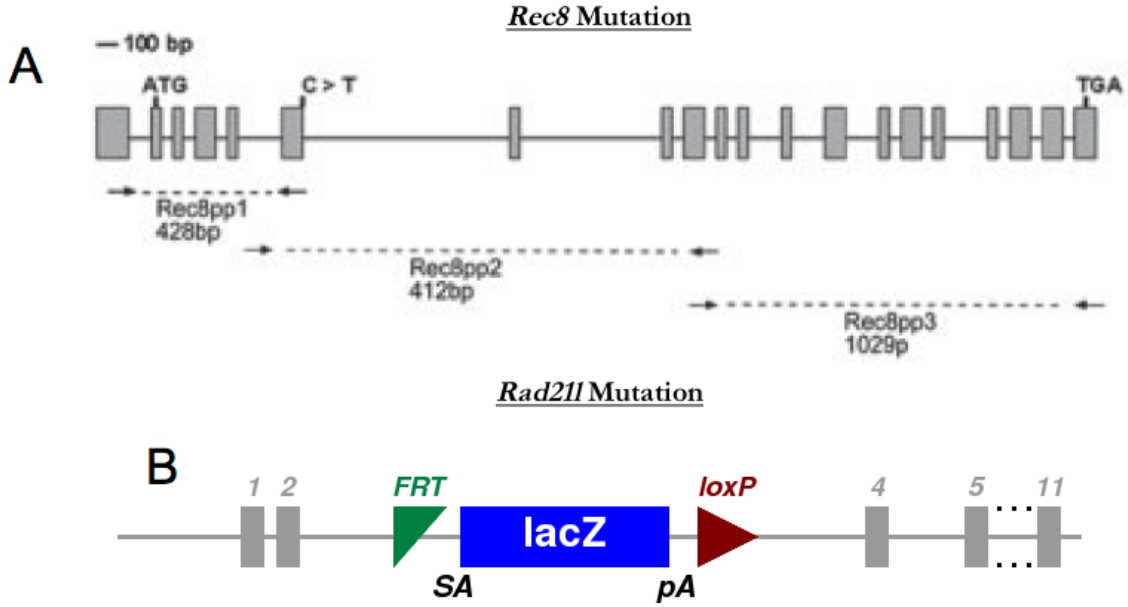

Figure 10: Two α-kleisin mutants used for this study. (A) Rec8 mutant allele: v6.4 ES cells, which are of the strain (C57BL/6Jx129S4/Jae) F1, with EMS [33]. (B) Rad21l mutant allele: C57BL/6N-derived JM8.N4 embryonic stem (ES) cells that were targeted with a β-galactosidase containing cassette that generated a knockout first reporter allele for Rad21l that harbored a floxed exon 3 were sourced from the International Knockout Mouse Consortium.

Chromatin Microspreads

Germ cell chromatin spreads were prepared as follows. Mice were first raised to age between days post-partum (DPP) 14.5 and DPP 20. Mice underwent cervical dislocation, and testis were dissected and placed in 1x Phosphate Buffered Saline (PBS). The tunica albicans was then removed, and the testis placed back into 1x PBS. The testes were then removed from solution and shredded (via microforceps) in Krebs-Ringer Bicarbonate Buffer (KRB) supplemented with protease inhibitor (PI) cocktail solution to liberate germ cells. Solution was then allowed to sit in 6 mL of this solution for 5 minutes. The solution was filtered through a 0.8 μm Nitex mesh, and centrifuged at 10,000 rpm for 5 minutes. Supernatant was discarded, replaced with 0.1M sucrose solution, and placed on slides incubated with 1% PFA solution (Electron Microscopy Sciences). Slides were allowed to sit for 2.5 hours, and washed with 1x PBS with Kodak Photoflo solution. Slides were allowed to air dry, and then washed 3x in wash buffer (1x PBS, Antibody Dilution Buffer (ADB). Primary antibody was then placed on slides, and allowed to incubate at 4 degrees Celsius over night. Solution compositions are shown below (Table 1).

Staining and Microscopy

Primary antibodies and dilution used are presented below (Table 2). Slides were first incubated in primary antibody diluted in antibody dilution buffer for 2.5 hours at room temperature. Immediately after this period, slides were rewashed in Photoflo solution, and the wash buffer steps repeated in preparation for secondary antibody incubation at 37 degrees Celsius for 2.5 hours. Secondary antibodies against human, rabbit, rat, mouse and guinea pig and conjugated to Alexa 488, 555, 568 or 633 (Life Technologies) were used at 1:500 dilution. Post incubation, slides were washed in 0.2% Photoflo in 1x PBS, and 0.2%

Photoflo in H_20 (PH8.0). Chromatin spreads were then mounted in Vectashield + DAPI medium (Vector Laboratories). Nuclear spread images were captured using a Zeiss CellObserver Z1 linked to an ORCA-Flash 4.0 CMOS camera (Hamamatsu).

Image Analysis

Images were analyzed with the Zeiss ZEN 2012 blue edition image software including foci and length measurement capabilities. Further analysis was completed using ImageJ software provided by the National Institutes of Health. Adobe Photoshop CS6 was used to prepare figure images. The .CZI proprietary format file exported from ZEN was opened in the ZEN software, yielding the captured chromosome spread (Fig.11). Using the image analysis tool, and selecting *Analyze Interactive*, we were able to both select the area of the spread to be quantified, the threshold of signal to be recognized by the system, and finally allowed to correct for any inconsistencies in signal recognition before a final length and quantity analysis was run by the program. The ZEN program was useful in analyzing the lengths of SYCP3 stretches, however when the lengths became much smaller in the mutant spermatocytes, the automatic recognition feature was turned off, and manual axis drawing/counting was done instead. For colocalization data, the colocalization function featured in the ZEN 2012 program allowed up to calculate the Manders coefficient of colocalization quite easily. 3 measures each were used of representative images, and the averages were then reported as the level of colocalization seen in each nuclear spread.

ImageJ was used to analyze the number of centromeres present in the chromatin spreads. The .CZI file was exported to a .tif format, and opening in the ImageJ program. As shown below (Fig.12), the program allowed us to use a manual cell counting tool to physically mark the centromeres on the exported image and presenting a sum upon

completion. This data was then exported to Microsoft Excel, and standard statistical analysis was run via GraphPad Prism6.

Table 1: Solutions and ingredients utilized in this experiment

A

Solution	Ingredients
Krebs-Ringer Bicarbonate (KRB) Media **Stock Solutions**	• 9% NaCL • 1.15% KCl • 6.5% $NaHCO_3$ • 2.1% KH_2PO_4 • 3.8% $MgSO_4*7H_2O$ • 1.2% $CaCl_2$ • 100X Penicillin-Streptomycin-Glutamine (Gibco cat no. 10378-016), aliquoted & stored at 20°C • 100X MEM Non-essential amino acids (Gibco cat no. 11140-050) • 50X MEM Essential amino acids (Gibco cat. No. 11130-051)
Krebs-Ringer Bicarbonate Media	• 39.0 mL of NaCL • 15.6 mL of KCl • 16.3 mL of $NaHCO_3$ • 3.9 mL of KH_2PO_4 • 3.9 mL of $MgSO_4*7H_2O$ • 5.9 mL of $CaCl_2$ • 5.0 mL of 100X Pen/Strep/Glu • 5.0 mL of 100X Non-essential aa • 50X MEM Essential amino acids

B

Solution	Ingredients
Sucrose (0.1M), 5mL	• 1 mL of 0.5M sucrose • 4 mL of MQ H_2O • 100 uL of 50mM NaOH (To bring the pH to 8.0) • 20 uL of 50x Protease Inhibitor Cocktail (Roche)
PFA (1%), 5mL	• 312.5 uL of 16% PFA • 4687.5 MQ H_2O • ~60 uL of NaOH (pH 8) • 20 uL of Protease Inhibitor Cocktail • 50 uL of 10% Triton X-100
Antibody dilution buffer (ADB)	• 50 mL PBS • 3% BSA • 10% goat or horse serum • 0.05% triton X-100
Washing/Blocking Buffer (WB) (10% ADB)	• 45 mL of PBS • 5 mL of 100% ADB

Table 2: Primary Antibodies used in this study

				Dilution
Antibody	Host	Source	Catalogue number	Immuno-fluorescence
CREST (CEN)	Human	Antibodies Incorporated	15-235	1:50
RAD21	Rabbit	Abcam	ab154769	1:250
RAD21L	Rabbit	Alberto Pendas	NA	1:250
REC8	Rabbit	Karen Schindler		1:500
SMC1α	Rabbit	Rolf Jessberger	NA	1:100
SMC1β	Rabbit	Rolf Jessberger	NA	1:250
SMC3 **STAG1**	Rabbit Goat	Abcam Abcam	ab9263 Ab4455	1:250 NA
STAG2	Goat	Santa Cruz	sc-54512	NA
SYCP1	Rabbit	Novus Biologicals	NB300-229	1:500
SYCP3	Rat	Mary Ann Handel	NA	1:500
SYCP3	Rabbit	Novus Biologicals	NB300-231	1:1000
SYCP3	Mouse	Santa Cruz	sc-74569	1:50
γH2AX	Mouse	Millipore	05-636	1:500

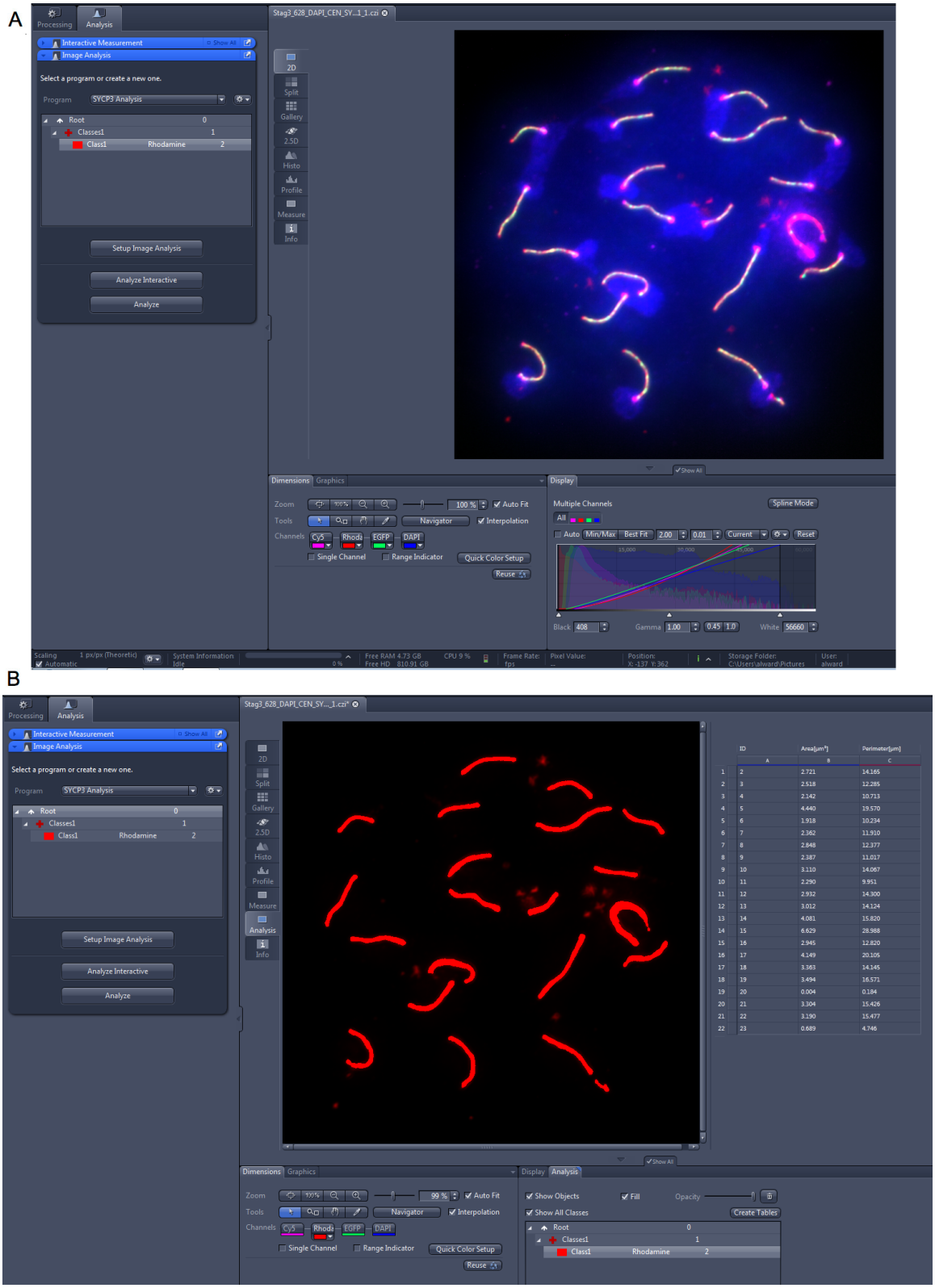

Figure 11: Images depicting the analysis of nuclear spreads via ZEN 2012 Image Software

A

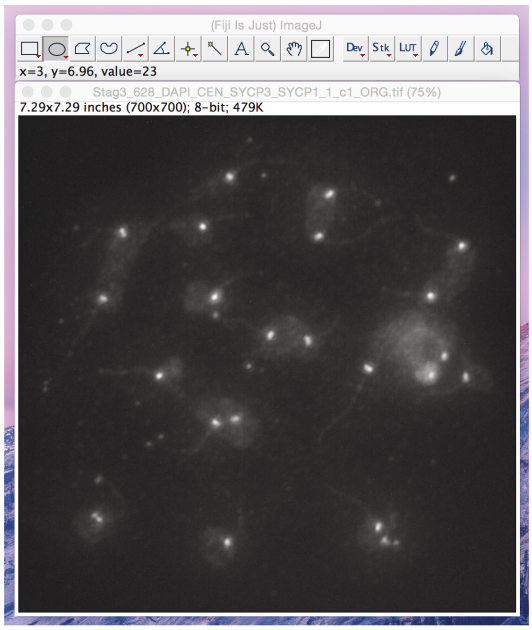

B

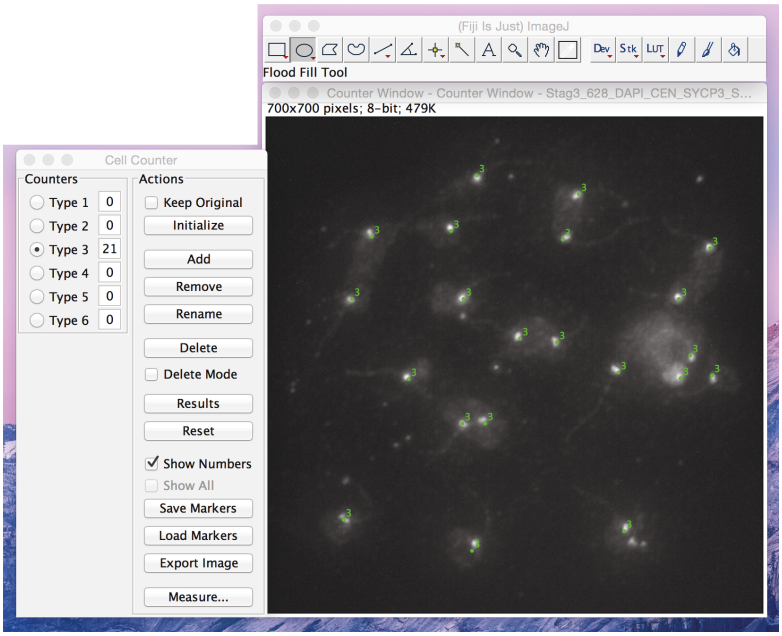

Figure 12 This illustration demonstrates the process by which the centromere signal was quantified in the chromatin spreads. The program ImageJ was used to manually count the number of centromeres present in each spread. (A) Depicts the raw image file before counting. (B) Depicts the image after counting has been completed.

Intended to be blank

RESULTS

Mutations in cohesin proteins leads to a zygotene-like arrest in male germ cells during meiotic prophase I

The SC is an essential structure for meiotic progression. Due to the temporal differences in accumulation of LEs and CEs to chromosomal axes, antibodies against proteins such as SYCP3 and SYCP1 can be used to stage the progression of prophase I. Wild type spreads in the earliest stage of prophase I (leptotene) show a large number of short stretches of SYCP3, with the absence of SYCP1. At the early zygotene stage, wild type spermatocytes show a reduced number of longer SYCP3 stretches. At this point SYCP1 begins to co-localize with SYCP3 indicating that homologous chromosomes have found each other and are beginning to synapse (Fig.13A, Supplementary Fig.S1) (avg. as reported by [6] for $Stag3^{+/Oy}$ control =43 SYCP3 stretches). Finally, during the pachytene stage the number of SYCP3 stretches decreases even more as autosomes synapse fully (Fig.13A-B, Supplementary Fig.S1) (avg. as reported by [6] for $Stag3^{+/Oy}$ control =20 stretches, N=50 nuclei). As the spermatocyte has progressed further through prophase I, the level of SYCP1 colocalization increases substantially (Fig.13A, Supplementary Fig.S1, SYCP3 in red, SYCP1 in green, colocalization in yellow). Localization of SYCP1 to the XY chromosome was intermittent, mainly seen at the aforementioned pseudo-autosomal region in assessed spermatocytes.

In the *Rad21l* and *Rec8* mutants, we observed stable colocalization of SYCP1 with SYCP3 axes. However, there was a noticeable decrease in the level of colocalization in the *Rad21l* as opposed to what seemed like normal levels of colocalization in the *Rec8* (Fig. 13A, Supplementary Fig.S1). The decrease seen in the *Rad21l* mutant coincided with the

characteristic zygotene-like arrest reported previously, where non-homologous chromosomes are abnormally associated [36] (Fig.13, Supplementary Fig.S1). The overall increase in axis number and decrease in axis length in the *Rec8* mutant is identical to the a zygotene like arrest previously reported [37] (Fig.13, Supplementary Fig.S1). Consistent with prior observations into the localization of SYCP1 in *Rec8* mutant spermatocytes, we observed fully co-localized regions of SYCP1/SYCP3. This has been hypothesized to be either the result of a complete SC-like structure being laid down between sister chromatids (rather than between homologous chromosomes) or incorrect pairing between two non-sister chromatids [37], [54]. More pronounced defects were observed in the *Stag3/Rad21l* and *Stag3/Rec8* double mutant mice. The *Stag3/Rec8* mutation showed more SYCP1 co-localization than the *Stag3/Rad21l*, albeit with shorter axis lengths and an increased axis number (Fig.13, Supplementary Fig.S1). Our final assessment in the *Rad21l/Rec8* mutation showed an almost non-existent colocalization of SYCP1 to SYCP3 labeled axes, consistent with previous findings (Fig.13A) [52].

Mutations in cohesin proteins increase the number of SYCP3 axes during meiotic prophase I

In wild type spermatocytes, completion of synapsis is noted by observing 19 fully synapsed autosomes and a partially synapsed X-Y chromosome pair (Fig.13A & C). When compared to the wild type, mutations in the meiosis specific α-kleisin genes *Rad21l* and *Rec8* resulted in an overall increase in the number of SYCP3 axes present during the stages of meiotic prophase I (Fig.13A & C, Supplementary Fig.S1). These increases resulted in averages of 31.84 and 40.58 axes, respectively. As previously described, the *Stag3* mutation

results in a zygotene-like arrest in mouse spermatocytes during meiotic prophase I, resulting a shorter length of SYCP3 axes in the spread nucleus of the spermatocyte. Confirming previous work, the spermatocytes cultivated in the presence of the stromal antigen protein *Stag3* homozygous mutation showed an average of 41 axes per spermatocyte (Fig.13 A & C; Supplementary Fig.S1). Finally, the presence of mutations in *Stag3 and* an α-kleisin resulted in significantly more axes per spermatocyte. In the *Stag3/Rad21l* spermatocytes, the average number of SYCP3 axes was 62.40, while in the *Stag3/Rec8* spermatocytes showed about 66.78 axes per nucleus.

Finally, we assessed the affect of combining mutations of both of the meiosis-specific α-kleisin subunits, *Rad21l* and *Rec8*. There are previous reports on the effect that these mutations have when combined in mouse models, however, no quantification of axes was performed [52]. The average number of axes present in our *Rad21l/Rec8* mutant was lower than those of the *Stag3/Rec8* and *Stag3/Rad21l* mutations, with an average axis number of to be 26.95 per spermatocyte (Fig.13).

Mutations in cohesin proteins decreases the overall length of SYCP3 axes during meiotic prophase I

Reported alongside the increase in number of axes was a decrease in the average length of the SYCP3 axes during meiotic prophase I. In our wild type spermatocytes, we measured an average length of 15.26 μm (at DPP=15). Mutation in either of the meiosis specific α-kleisins *Rad21l* and *Rec8* resulted in a marked decrease in the length of SYCP3 axes present during the stages of meiotic prophase I. While the *Rad21l* mutation resulted in axes

of average length of 9.48 μm, the *Rec8* mutation resulted in two distinct length populations, one of average length 7.36 μm, and a second with an average length of 18.61μm (Fig.13A-B, Supplementary Fig.S1). The observation of distinct populations of *Rec8* spermatocytes is consistent with several observations as to the nature of the *Rec8* mutation in mouse spermatocytes [34], [37], [54]. The *Stag3* mutation resulted in a concentrated average length of 5.29μm. The presence of mutations in *Stag3 and* an α-kleisin protein resulted in significantly shorter axes per spermatocyte. In the *Stag3/Rad21l* spermatocytes, the average length of SYCP3 axes was 3.04 μm, while in the *Stag3/Rec8* spermatocytes showed 1.87 μm axes per nucleus. This resulted in a roughly inverse relation between axis length and axis number in wild type and mutant spermatocytes.

Finally, we assessed of the effect of combining mutations of the two meiosis-specific α-kleisin subunits, *Rad21l* and *Rec8*. Again, no quantification of axes had been previously performed. Our microspread nuclei showed an average length of axes present in the *Rad21l/Rec8* double mutant to be similar to those of the *Stag3/Rec8* mutation, but almost half the length of the *Stag3/Rad21l* mutation. The average length of axes was calculated to be 1.76μm per spermatocyte (DPP=15).

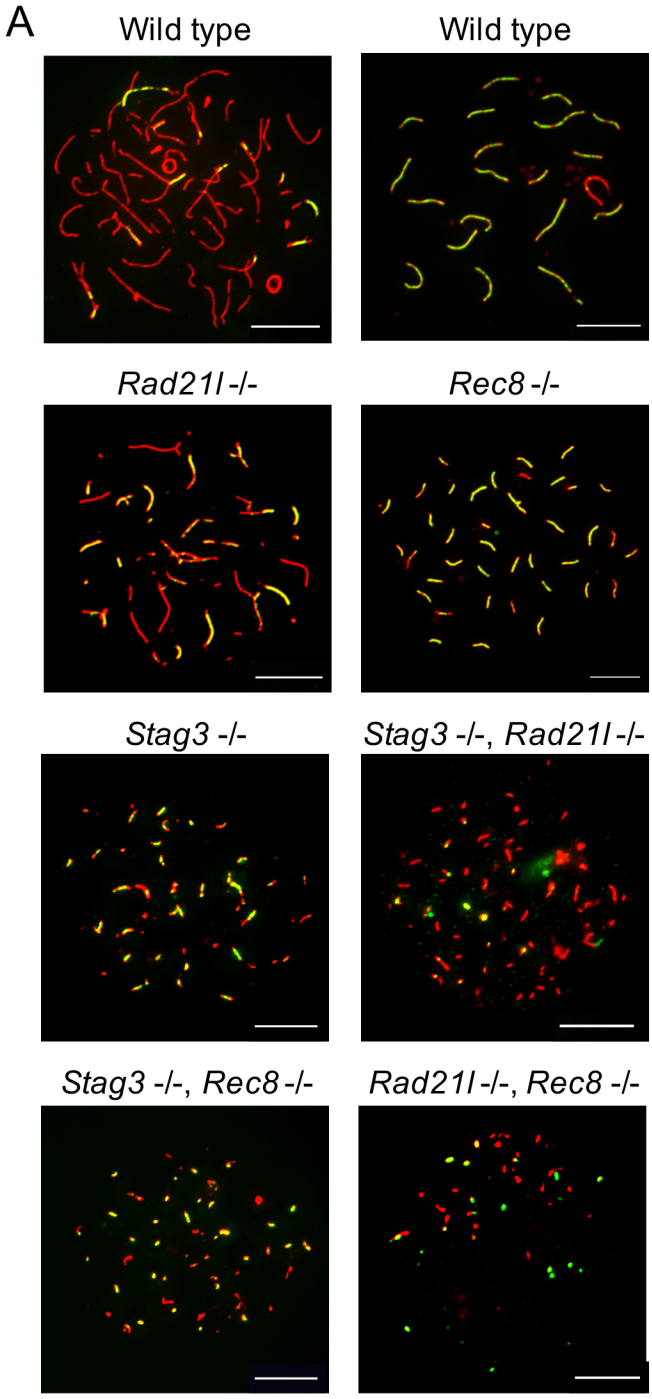

Figure 13: Microscopy and Analysis of SYCP3 localization in meiotic prophase I. (A) Microscopy of DPP=15 mouse chromatin spreads acquired from the testis. Images show SYCP3 (Red) localization to the chromosome axes, and colocalization of SYCP1 (green) to these same axes as a mark of progression through prophase. Areas of colocalization appear yellow in color. All scale bars set to 10 μm.

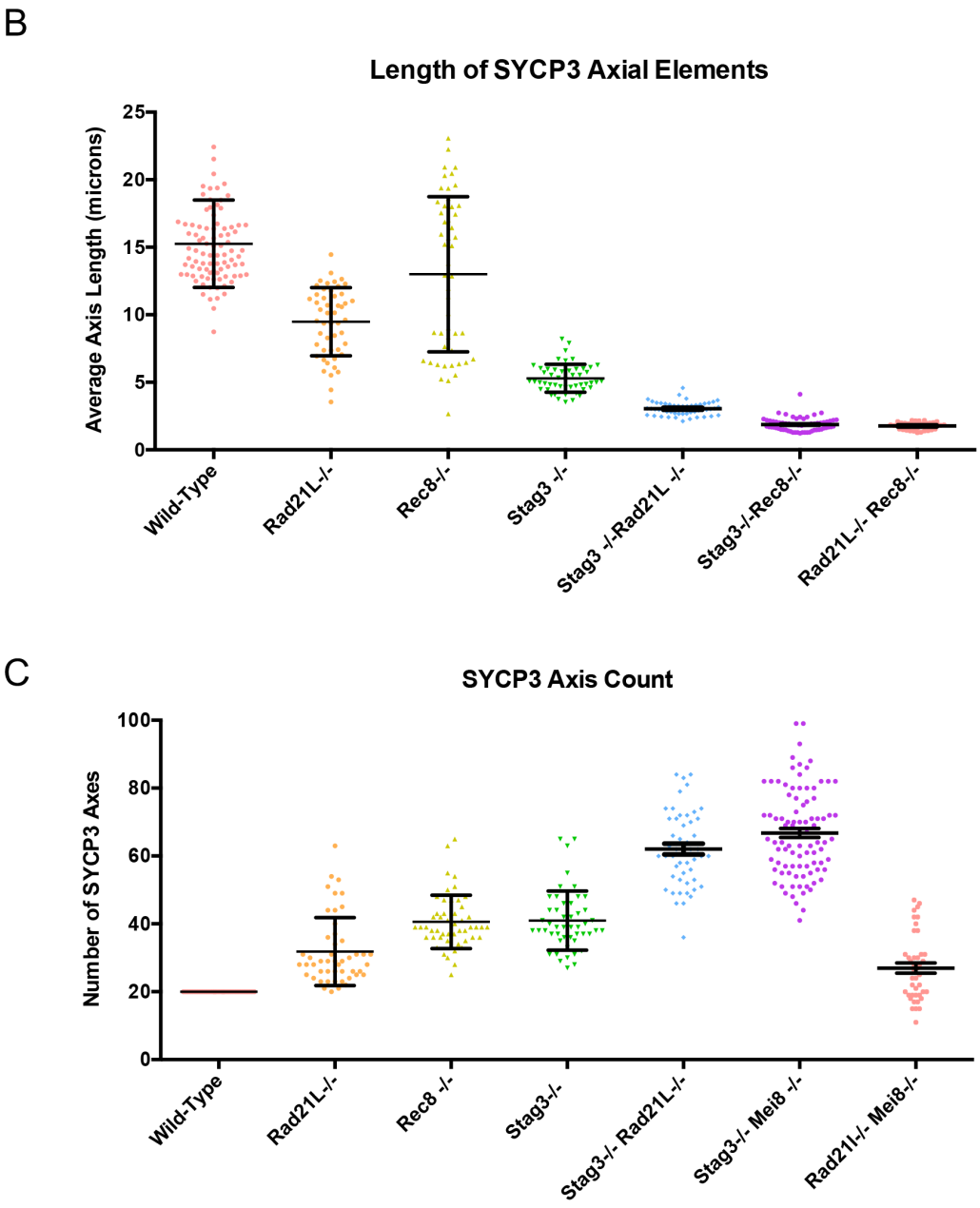

Figure 13: Microscopy and Analysis of SYCP3 localization in meiotic prophase I. (B) Analysis of axis length in chromatin spreads during meiotic prophase I (n=50). (C) Analysis of the number of SYCP3 stained axes present in meiotic prophase I. The X axis shows the genotype in (B) and (C) (n=50). All scale bars set to 10 μm.

Mutations in cohesin proteins lead to an increase in centromere signal

The centromere is an important structure during prophase I, as it is responsible for many of the early chromatin dynamics that take place at the beginning of and throughout prophase I. In wild-type chromatin spreads, the spermatocytes presented with a normal number centromere-kinetochore signal (one per axis) giving an average of 21 signals present per spread (Fig.14A-B, Supplementary Fig.S2). This number increased in the zygotene preparation compared to the pachytene, which corroborates the fact that synapsis ends with the centromere-kinetochore proximal end of the homologues [55]. However, in the mutations specific for the meiosis specific α-kleisin subunits*Rad21l* and *Rec8*, we see an increase in the centromere-kinetochore signal that is proportional to the increase in number of SYCP3 axes in similar mutants (averages of 29.87 and 42.74 centromeres, respectively). This data is indicative of incomplete synapsis between homologues, and predictably shows an increase in centromere-kinetochore signal in the *Rec8* mutant likely due to REC8 involvement in centromeric cohesion [37]. In the *Stag3* mutant, we see a similar increase in the number of centromere-kinetochore signal in the zygotene-like arrest phase, displaying an average of 41.92 signals per spread. This trend continued with the *Stag3/Rad21l* and *Stag3/Rec8* mutants. As shown in Figure 14 (trend corroborated in Supplementary Fig.S2), we observed an increase to an average of 44.46 signal per spread for the *Stag3/Rad21l* mutant, and 65.29 signals for the *Stag3/Rec8* mutant. Interestingly, the *Rad21l/Rec8* mutant showed an overall decrease in centromere-kinetochore signal, with an average of 15.96 signals per spread (Fig.14).

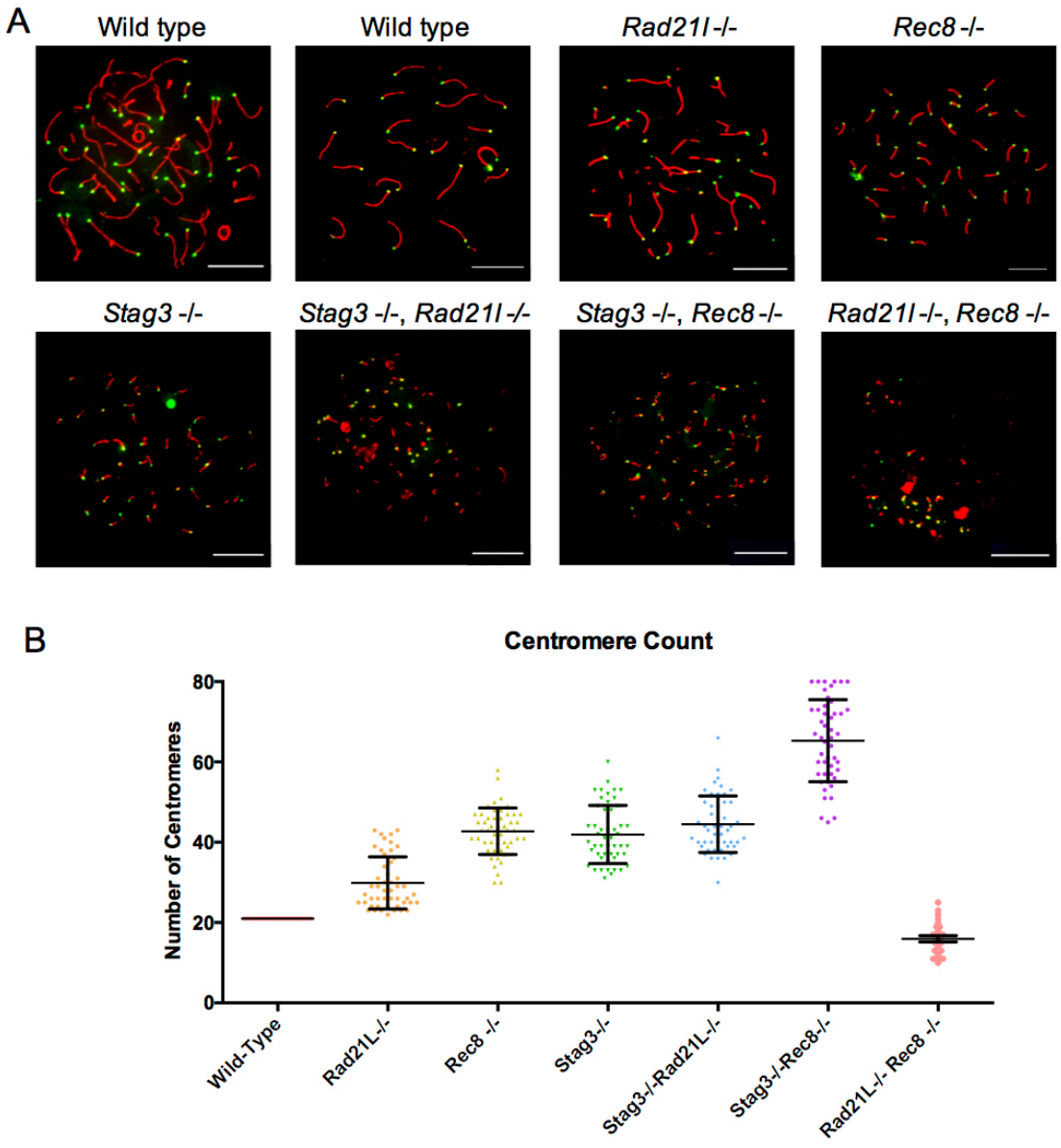

Figure 14: Centromere Microscopy. (A) Images showing colocalization of SYCP3 (red) and Centromere (green). (B) Quantification of the average number of centromere signals counted in each individual spread (n=50). The Y axis depicts the genotype of the spreads in question. All scale bars set to 10 μm.

Protein Localization is Altered by Mutations in Cohesin Complex Proteins

There are six known forms of the cohesin complex that exist between mitosis and meiosis, made up of different combinations of the SA, α-kleisin, and SMC proteins. In wild-type spermatocytes, we observed the presence of SMC3, RAD21, RAD21L, REC8, SMC1α, and SMC1β co-localizing to the chromosomal axis in both zygotene and pachytene chromatin spreads. However, availability of cohesins was altered in mutant preparations compared to WT. In chromatin spreads prepared with immunostaining for RAD21 and SMC3 we observed little to no change between the localization of the protein to the SYCP3 stained axes (Fig.15-16). The following sections describe the observations by mutation.

Rad21l, Rec8, and Stag3 Mutants

As negative controls, we stained the *Rad21L* and *Rec8* mutants for the RAD21L and REC8 proteins respectively. As expected, these proteins did not localize to the SYCP3 stained axes of the chromatin spreads, with Manders coefficients of 0.39 and 0.50 respectively (Fig.15 B-C). In all other preparations there appears to be a decrease in the localization of meiotic cohesin complexes to the SYCP3 stained chromosomal axes, commensurate with the hypothesis that the same cohesin destabilization that is seen with the *Stag3* mutation is present in the mutations of other meiosis specific cohesin components. In the *Stag3* mutant chromatin spreads, this same destabilization of cohesin was observed, showing a smaller level of co-localization of each cohesin complex protein. These proteins were observed to have a Manders coefficient of 0.75 and 0.75, respectively. This is compared to 0.95 in the wild type pachytene spreads(Fig.15-16).

Stag3/Rad21l and Stag3/Rec8 Mutants

In the *Stag3/Rad21l* mutation, there was a stark decrease in the localization of cohesin complex proteins to the axes. In these chromatin spreads, we see that while there is an obvious absence of RAD21L localization to the chromosome axes with SYCP3 (Manders=0.44), we still see the decrease in other cohesin components, namely REC8 and and SMC1β (Manders=0.85 and 0.61, WT values of 0.95 and 0.87 respectively). In the case of the *Stag3/Rec8* mutation, we see localization of SMC3, REC8, SMC1A and SMC1B to the axes, with a lower level of colocalization for SMC1B and the absence of REC8 colocalization to SYCP3 axes (Fig.16). These proteins had Manders colocalization coefficients of 0.99, 0.59, 0.80, 0.61 respectively.

Rad21l/Rec8 Mutants

Previous data has suggested that while there are still visible chromosomal axes present in the *Rad21l/Rec8* mutant, that these axes are short and few in number [52]. Our observations of the mutant via immunofluorescence microscopy were consistent with this result. We observed highly reduced colocalization of the RAD21 (Manders=0.8, vs 0.98 in WT) and SMC3 (Manders=0.68) antibodies to the SYCP3 axes, but noticed the apparent absence of SMC1α (Manders=0.79) and SMC1β (0.54) from axes. Naturally, the RAD21L (Manders= 0.57) and REC8 (Manders=0.56) proteins were missing from axes as well. This mutation was the most severe phenotype when compared to all prior mutations reported in this section.

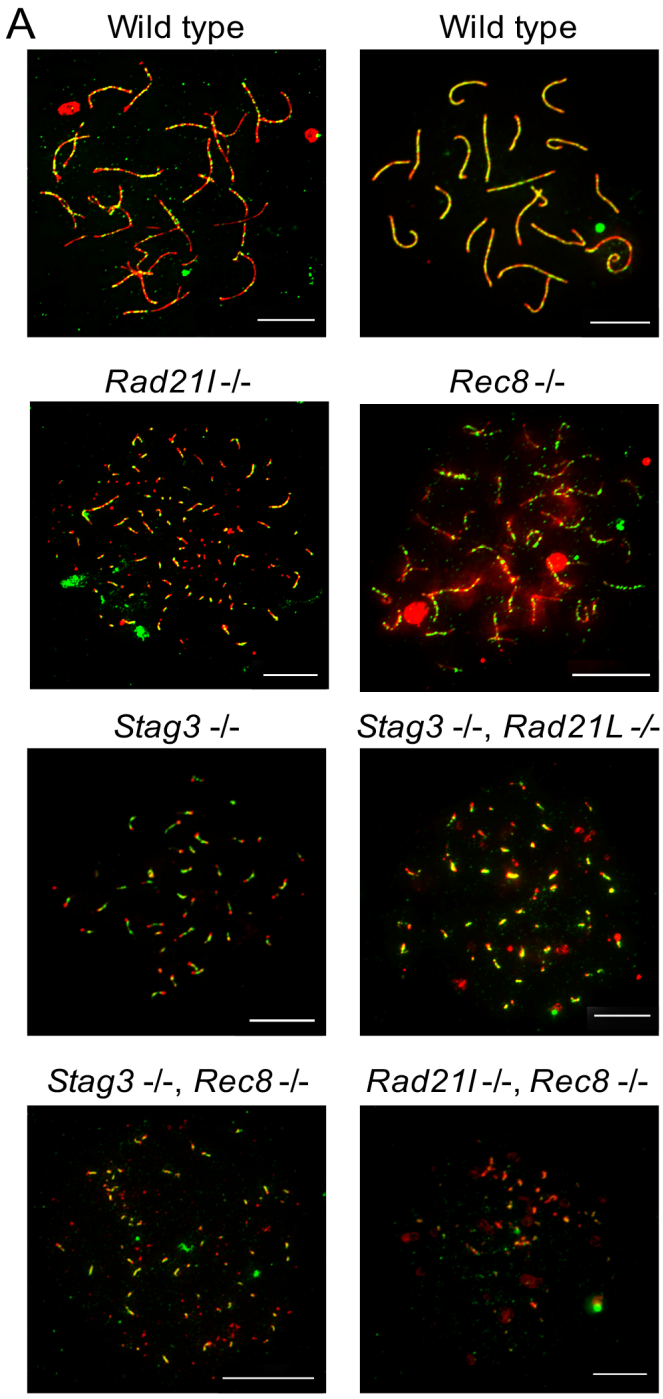

Figure 15: Localization of cohesin complex proteins on SYCP3 stained chromosomal axes. SYCP3 is depicted in red, Cohesins in green. (A) Imaging of SYCP3 co-localization with RAD21 (green). All scale bars set to 10 μm.

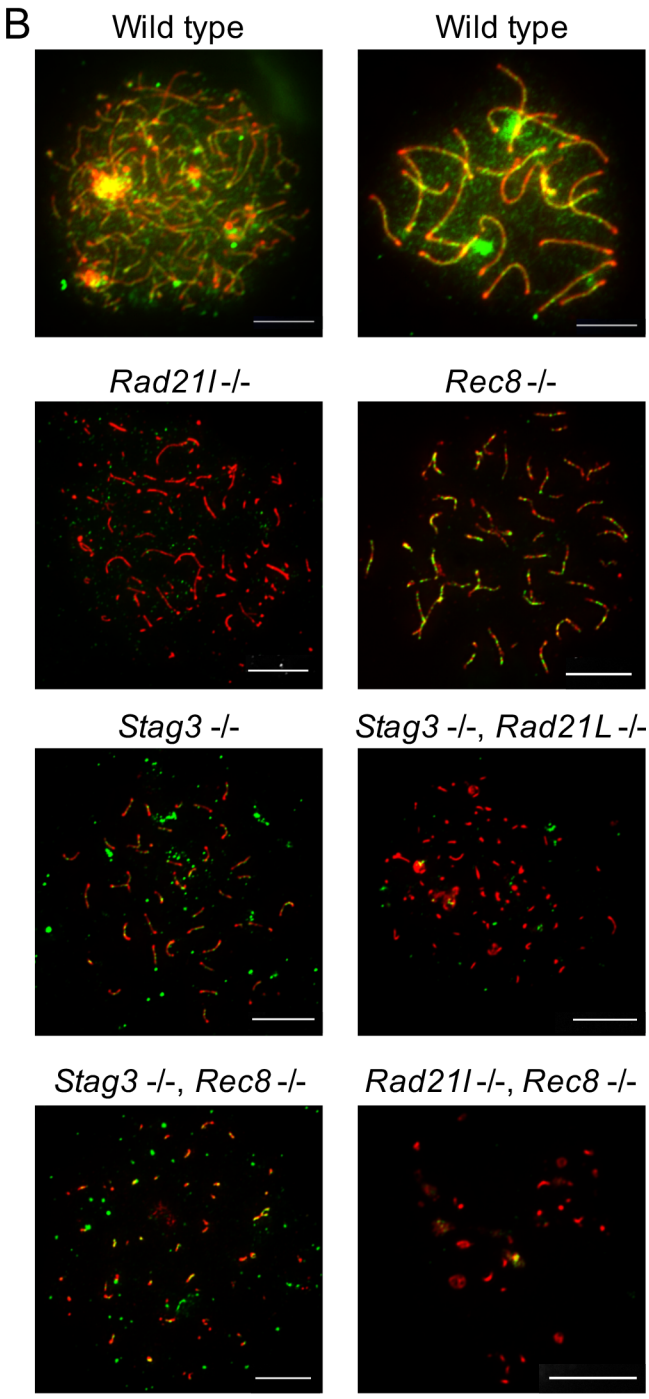

Figure 15: Localization of cohesin complex proteins on SYCP3 stained chromosomal axes. SYCP3 is depicted in red, Cohesins in green. (B) Imaging of SYCP3 co-localization with RAD21L (green). All scale bars set to 10 μm.

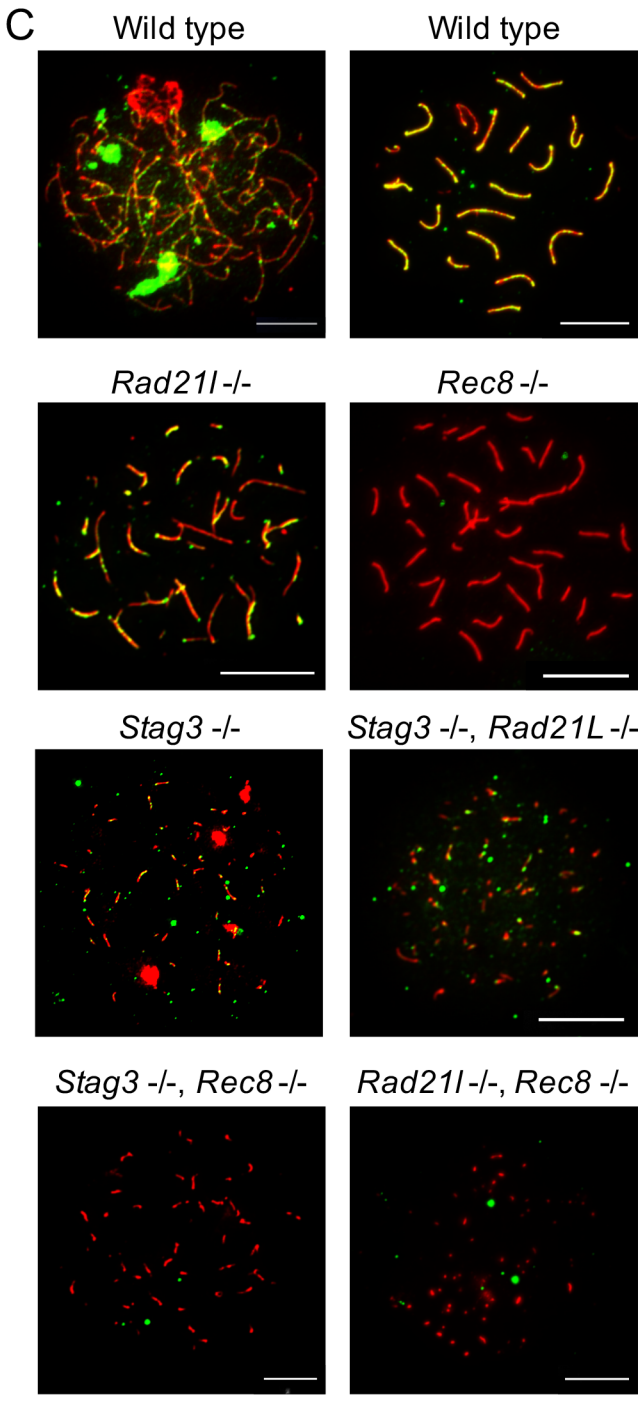

Figure 15: Localization of cohesin complex proteins on SYCP3 stained chromosomal axes. SYCP3 is depicted in red, Cohesins in green. (C) Imaging of SYCP3 co-localization with REC8 (green).

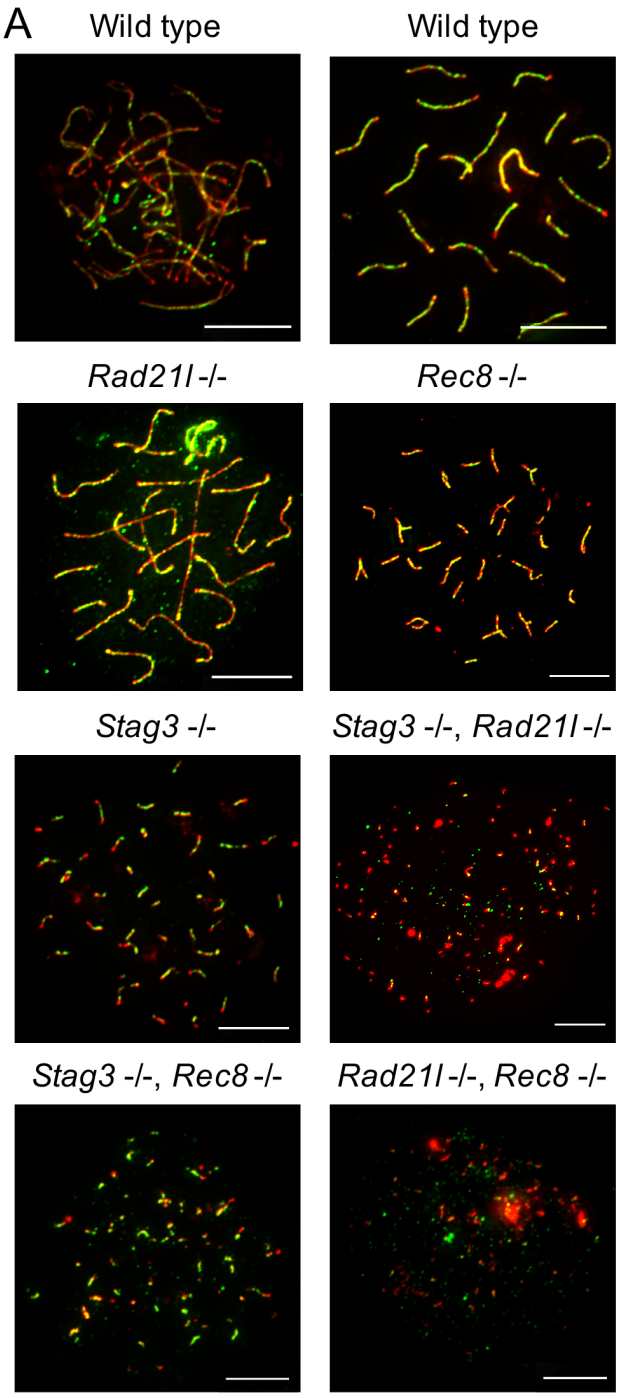

Figure 16: Localization of cohesin complex proteins on SYCP3 stained chromosomal axes. SYCP3 is depicted in red, Cohesins in green. (A) Imaging of SYCP3 co-localization with SMC3 (green). All scale bars set to 10 μm.

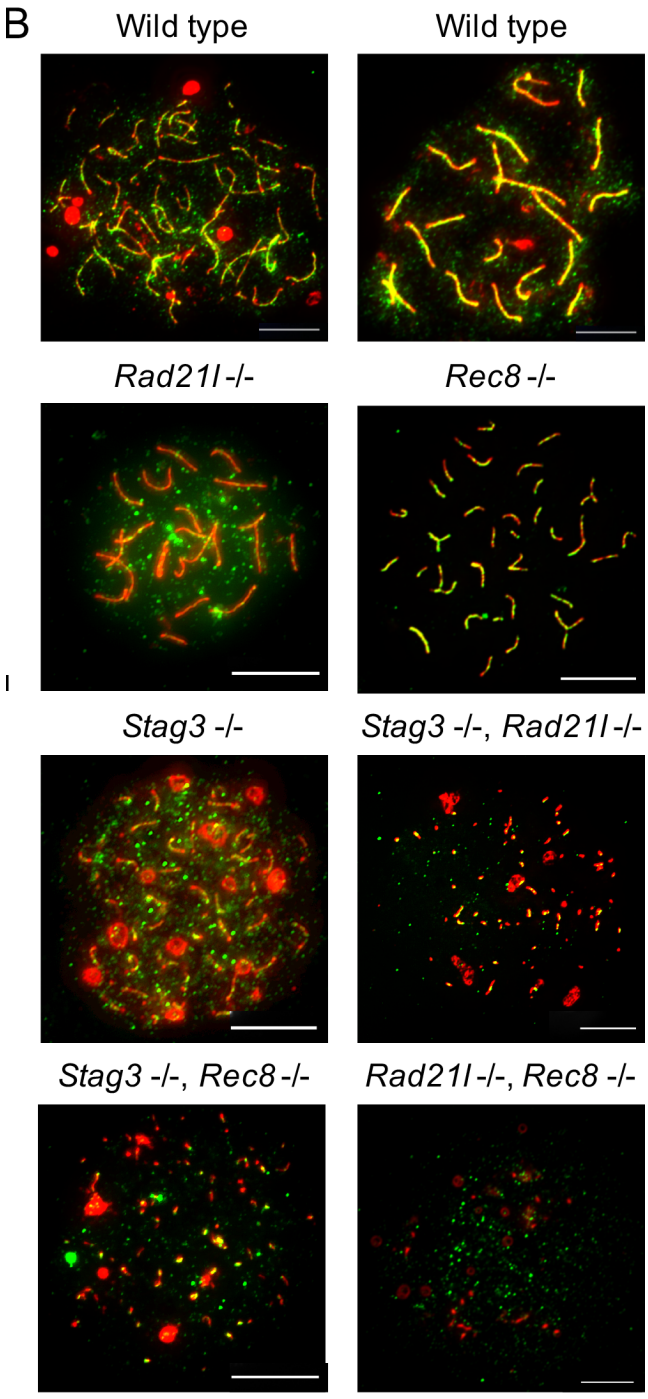

Figure 16: Localization of cohesin complex proteins on SYCP3 stained chromosomal axes. SYCP3 is depicted in red, Cohesins in green. (B) Imaging of SYCP3 co-localization with SMC1A (green). All scale bars set to 10 μm.

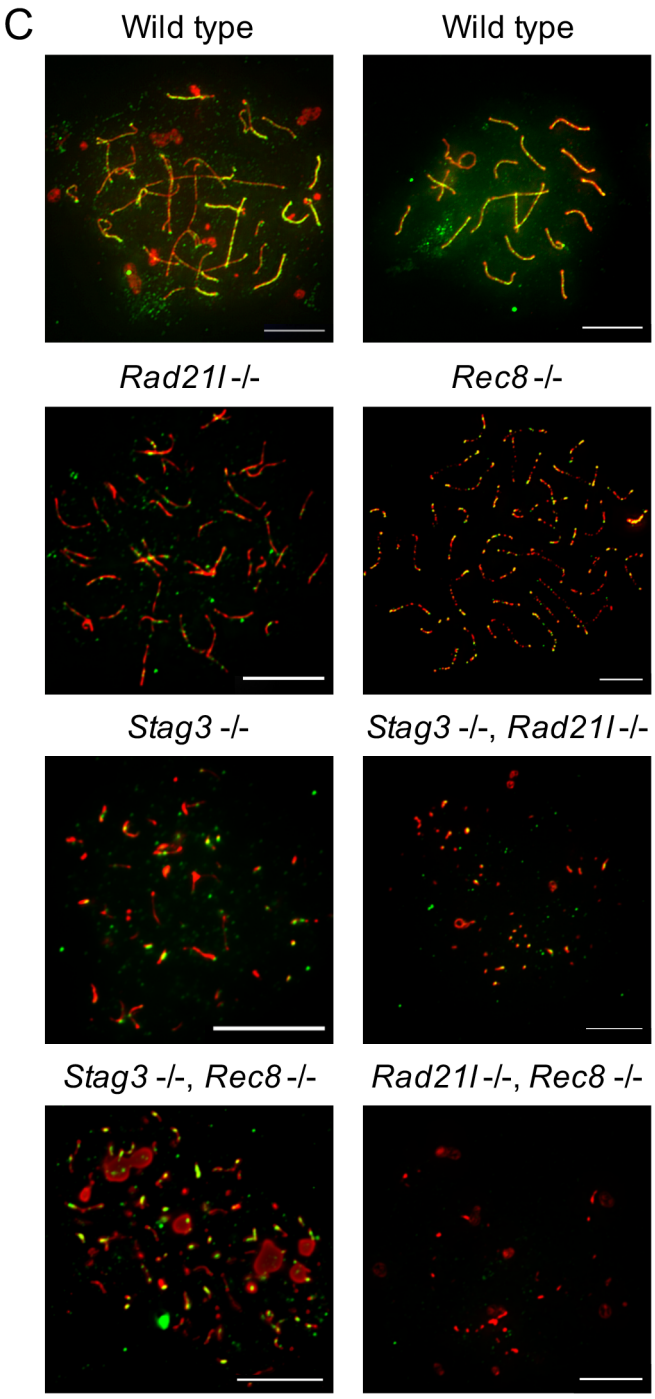

Figure 16: Localization of cohesin complex proteins on SYCP3 stained chromosomal axes. SYCP3 is depicted in red, Cohesins in green. (C) Imaging of SYCP3 co-localization with SMC1B (green). All scale bars set to 10 μm.

Analysis of Chromosome Dynamics during Prophase I

Various interaction studies have indicated that cohesin components first localize to chromosomal axes during the pre-leptotene stage [30-31] [36-39], [56]. Many other processes important to the chromosome movements that take place during prophase are regulated by this association. Telomeres also become associated with the nuclear envelope at this stage, and this interaction is crucial to facilitate chromosomal movements at the beginning of prophase I [57]. Prior work has shown that meiosis specific cohesin complexes co-localize with telomeres, and the interaction is required to stabilize the telomeric interaction with the nuclear periphery [10]. Recently, it has been shown that mutants for telomere associated protein Telomere Repeats-Binding Bouquet Formation Protein 1 (TERB1) show defects in the ability to localize cohesin components [58]. Furthermore, this telomere associated protein has been shown to interact with STAG3 in spermatocytes. TERB1 interacts with the SUN domain-containing protein 1 Protein KASH5 (SUN-KASH) complex, which is important for telomere attachment to the nuclear periphery [58]. Therefore, we hypothesize that the *Stag3* mutant will have defects in telomere-nuclear periphery attachment. It is important to note that mouse chromosomes are telocentric, and we see a colocalization of centromere and telomere at one end of the chromosome. Due to this localization, it is possible to use immunofluorescence of the centromere to visualize the level of chromosome attachment to the nuclear periphery. Given the interdependency of the cohesin complex and telomeres for adequate meiotic progression, we attempted to visualize the associations between the chromosomal axes, centromere, and the nuclear periphery in both wild type and *Stag3* mutant spermatocytes (Fig.17). Our observations in the WT spermatocytes showed a

consistent localization of the centromere to the nuclear periphery, consistent with findings by Watanabe et al [58]. However, in the *Stag3* mutant spermatocytes we saw an increase in the centrally localized centromeric signal, indicating aberrant association with the nuclear periphery. To ensure that the reported signal was not misinterpreting the three-dimensional nature of the nucleus, we used a 3D reconstructive model to visualize these results, shown in Fig.17. These show a difference both in the density of the 3D representation of the WT vs *Stag3* mutant, with the characteristic short numerous axes represented clearly (Fig.17B) These results are in line with other meiosis specific cohesin mutations, and their effect on centromere cohesion [6], [58].

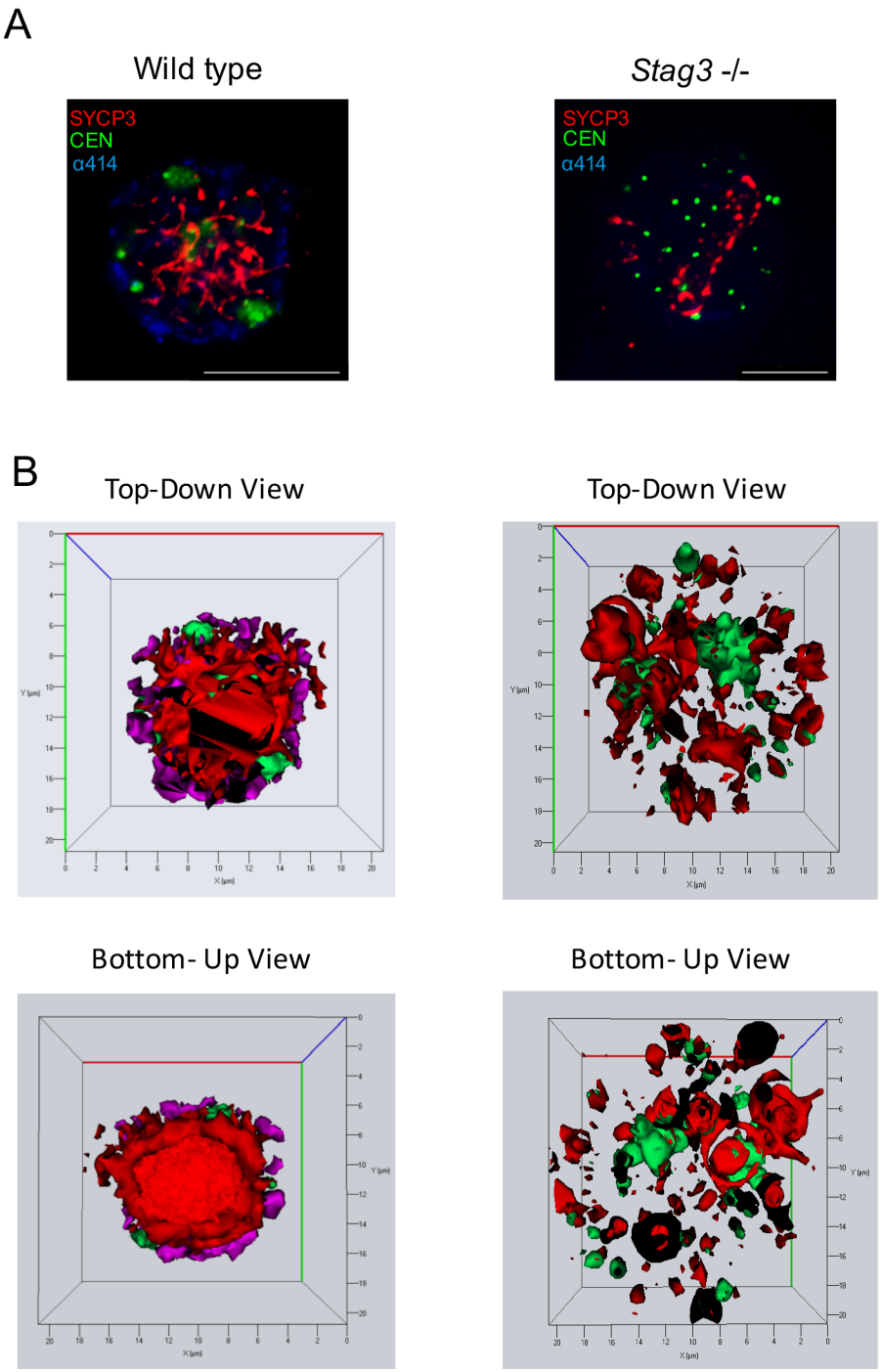

Figure 17: 3 dimensional deposition, imaging, and reconstruction model made using the ZEN 2012 program. (A) Immunofluoresence illustrating the difference in localization of centromere (green)s, WT towards periphery and Stag3 towards the interior. Nuclei were also stained with SYCP3 (red). (B) 3D reconstructed model showing depth and localization of centromeres and SYCP3 in the intact nucleus. All scale bars set to 10 μm.

Mutations in cohesin proteins leads to variations in pericentromeric heterochromatin clustering

As was previously stated, we know that cohesin complexes first localize to chromosome axes during the pre-leptotene stage of meiotic prophase I [6], [33-34]. However, this association is much more specific. Cohesin complexes containing REC8 and RAD21L generally localize to the chromatin arms, but also localize to chromatin areas near the centromere. Cohesion at pericentromeric regions throughout meiosis I is essential for the correct reductional segregation of sisters in the following meiosis II, and as such must be protected. Associations between the kinetochores at the centromere core regions can help maintain monopolar attachments during meiosis I. Given how important it is to maintain fidelity in these pericentromeric areas, they also contain a large amount of heterochromatin, known as pericentromeric heterochromatin that tend to cluster together to form "chromoclusters" [6]. These areas serve an important role in suppressing meiotic recombination in the surrounding areas of the chromosomes. Recombination in these areas can lead to branched chromosome structures and formation of chiasmata at incorrect areas leading to meiotic segregation errors. Furthermore, as previously discussed, associations between the centromere and telomere to the nuclear periphery are important for chromosome dynamics in early prophase I, indicating an interdependency between the pericentromeric heterochromatin and cohesin complex in the early pairing of chromosomes and directing areas of homologous recombination.

In nuclear spreads, it is easy to identify chromocenters, generally they appear as highly dense areas of DAPI staining. In wild type zygotene spreads, we observed an average of 11.88 chromocenters per nucleus, and an overall ratio of 1.76 centromeres per

chromocenters (Fig.18). In the *Rec8* -/- and *Stag3* -/- mutant, we observed 18.72 and 18.76 chromocenters per nucleus, respectively. In the *Rad21l* -/- mutant, we observed a stark decrease in the number of chromocenters per nucleus, with an average of 3.4 (ratio: 8.76). Interestingly enough, there was also a visible increase in the size of the chromocenters in the *Rad21l* -/- mutants when compared to other mutants. In the *Stag3*/*Rad21l* mutant spermatocytes, we observed an average of 8.4 chromocenters, while we observed 23.88 in the *Stag3*/*Rec8* mutants (Fig.18). These each showed a centromere:chromocenter ratio of 5.53 and 2.73, respectively. The observation of larger chromocenters persisted into the *Stag3*/*Rad21l* mutant as well, when compared to the *Stag3*/*Rec8* mutant. Finally, the *Rad21l*/*Rec8* mutant showed an average of 3.4 chromocenters per nuclear spread. However, the ratio of centromeres to chromocenters was 4.69, indicating that while there were a similar number of chromocenters in the *Rad21l*/*Rec8* when compared to the *Rad21l* mutant, the *Rad21l*/*Rec8* mutant contained fewer centromere signals per chromocenters (Fig.18).

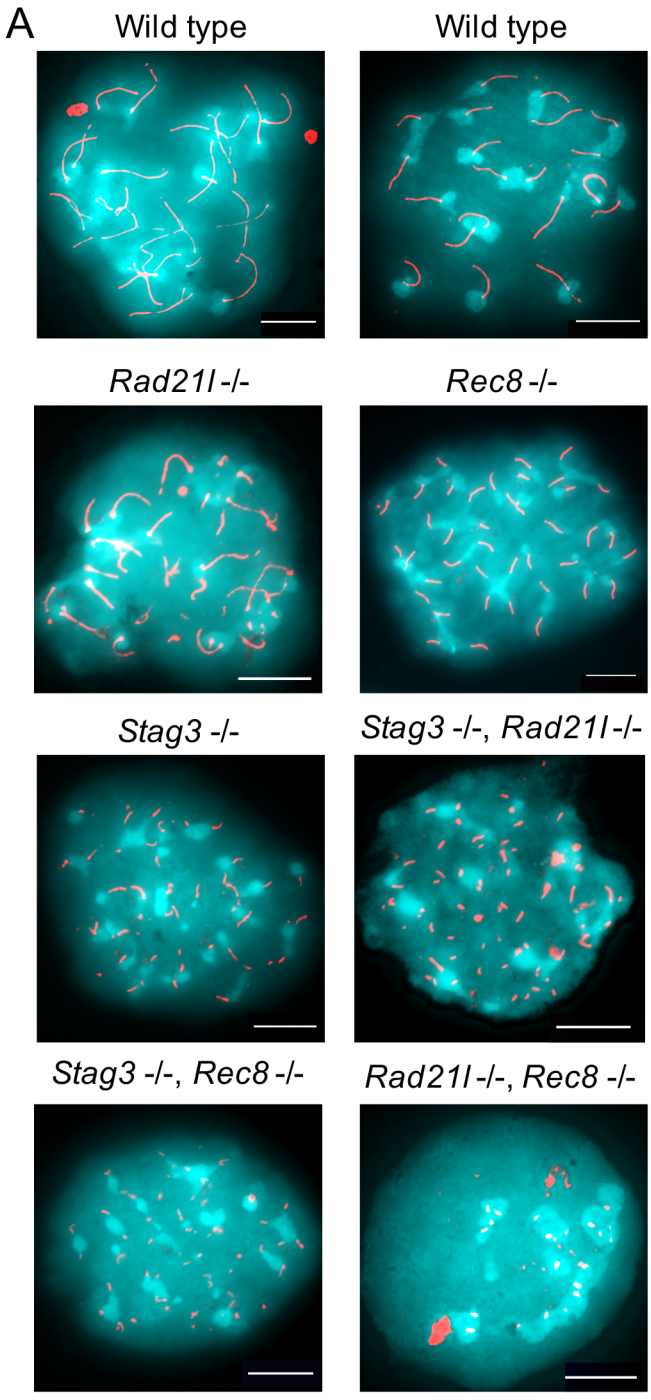

Figure 18: Analysis of pericentromeric heterochromatin. (A) Immunofluorescence microscopy detailing the localization of pericentromereic heterochromatin in nuclear spreads stained with SYCP3 (red) and DAPI (turquoise). All scale bars set to 10 μm.

B

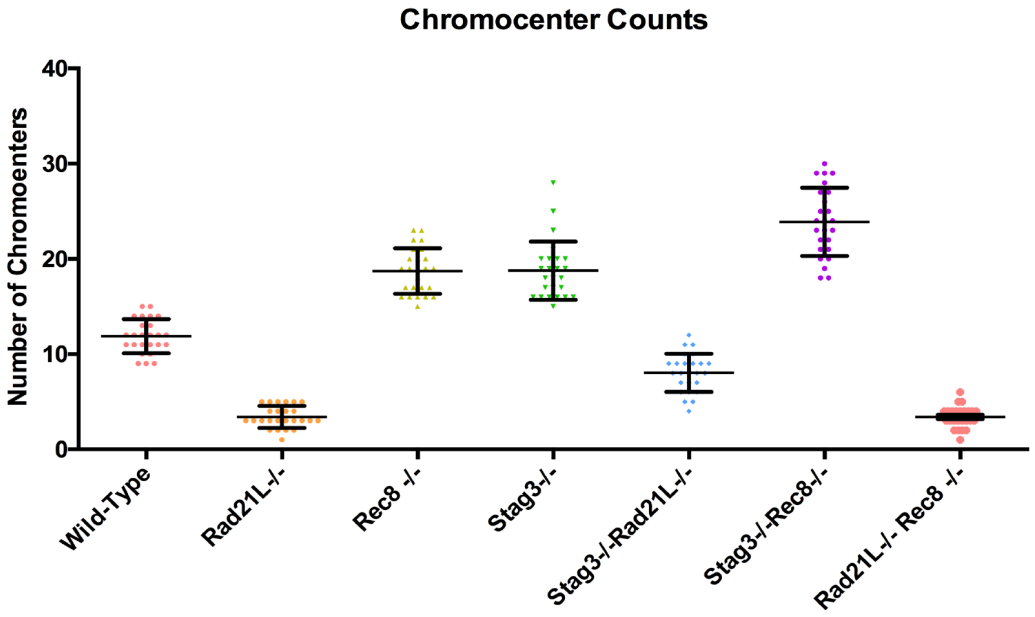

C

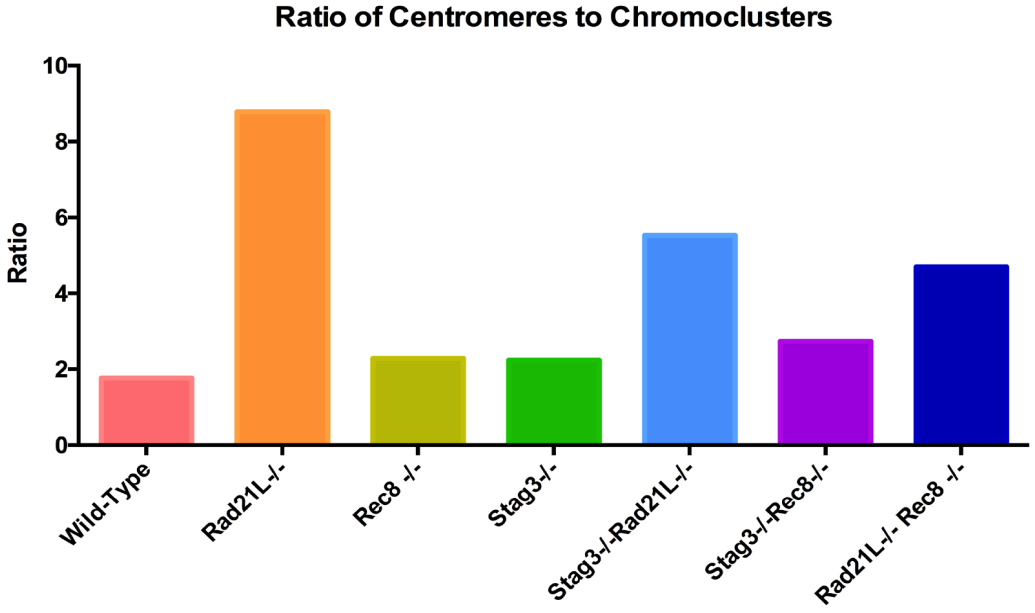

Figure 18: Analysis of pericentromeric heterochromatin. (B) Quantification of the number of pericentric heterochromatin clusters present in nuclear spreads (N=25). (C) Graph depicting the ratio of centromere signals to chromocenters clusters.

This page is meant to be blank

DISCUSSION

α-kleisins and the development of the SC

Recent investigations by our lab and others have indicated the necessity of STAG3 for the stability of meiotic cohesin complexes [6], [13], [59-60]. However, the reduced severity of the phenotype when compared to *Rad21l/Rec8* double mutants called into question its necessity [52]. We began with the characterization of *Rad21l* and *Rec8*. In the *Rad21l* mutant we observed that there was indeed a zygotene-like arrest in meiotic progression. Our spreads exhibit incomplete synapsis between homologous pairs, as well as a degree of synapsis between non-homologous chromosomes, resulting in mismatched pairs (Fig.13A). In repair of SPO11-induced DSB's, we observed that there was widespread γH2AX, indicating that the absence of RAD21L causes to an inability to repair DSBs, resulting in a DNA damage phenotype that highly resembled that of a zygotene stage spermatocyte (Supplementary Fig.S3). It has been suggested that RAD21L is important for the the initiation of homologue pairing in prophase I, and our results are consistent with that finding [27]. Our *Rec8* mutant also exhibited a zygotene-like arrest, though it showed more consistent SYCP1 localization than the *Rad21l* mutant (Fig.13A). However, synapsis in this mutant is incorrect SC localization between sister chromatids, as opposed to between homologous chromosomes as it is in the wild type spermatocytes [37], [54]. Although there is an increased level of synapsis when compared to the *Rad21l* mutant, we still witnessed a similar level of unrepaired DSBs in the *Rec8* mutant, indicating that SC formation between sisters is not sufficient for DNA repair (Supplementary Fig.S3). Our nuclear spreads from *Stag3* mutants clearly corroborate our prior results, showing a defect in chromatid cohesion (Fig.13, Supplementary Fig.1), defects in centromere cohesion (Fig. 14, Supplementary Fig.2),

SC formation between sister chromatids, and an increase in unrepaired DSBs (Supplementary Fig.3). These results give credence to the importance of STAG3 in stabilizing the cohesin complex during meiosis, and set the stage for the analysis of the double mutants.

In order to determine the true nature of STAG3's role, we generated and analyzed *Stag3/Rad21l, Stag3/Rec8* and *Rad21l/Rec8* double mutants. When characterizing these mutants, we observed each of the *Stag3* phenotypes, coupled with the phenotypes observed within the individual *Rad21l* and *Rec8* counterparts. Both the *Stag3/Rad21l* and *Stag3/Rec8* mutants showed the characteristic zygotene-like arrest that was witnessed in the *Stag3* mutant (Fig.13A). While both of these mutants were able to form AEs, the *Stag3/Rad21l* mutant was much less able to form the full SC, as shown by the extreme loss of SYCP1 at chromosomal axes (Fig.13A). The *Stag3/Rec8* mutant, on the other hand, maintained SYCP1 localization, though at a much lower level than the *Rec8* single mutant. Each mutant showed an increase in the gross number of SYCP3 labeled axes, and a decrease in the length of each axis (Fig.13B-C), indicating that the *Stag3* mutation was inducing additional instability in the localization of SC components to chromosome axes. This result is in line with our hypothesis. The *Stag3* mutation exhibits a more severe phenotype than the *Rad21l* and *Rec8* mutants alone. The fact that *Rad21l*, and *Rec8* mutants show distinct phenotypes, and gain *Stag3* specific phenotypes in the double mutant, rather than an exacerbation of previous phenotypes is interesting. It indicates STAG3's necessity for stabilization of the meiotic cohesin, and distinguishes the function between the STAG proteins and the α-kleisins.

When comparing the double mutants (*Stag3/Rad21l* and *Stag3/Rec8*) it is immediately apparent that the phenotypes they present are less severe than that of the *Rad21l/Rec8*

double mutant (Fig.13). While it is noticeable that there are marked defects in centromeric cohesin, it is clear that there is a distinct lack of chromosomal axes in this mutant. The axes observed have not aggregated SYCP1, and thus the SC has not commenced formation (Fig.13). This phenotype, unlike the *Stag3/Rad21l* and *Stag3/Rec8* mutants, does not appear to be a happy medium between the two individual mutations; rather, it is a distinct and separate phenotype, one showing an inability to form axes. This result is striking, and it lends itself to the idea that the α-kleisin proteins may be the ones necessary for axial element formation, and that STAG3 stabilizes this interaction. The axes that are still formed co-localize with RAD21 containing cohesins. It has already been observed that a temporal balance exists between cohesin complexes during meiosis (Fig.19). It may be that a balance between RAD21, RAD21L, and REC8 is necessary for correct axis formation during early leptotene stage, with STAG3 stabilizing each of these cohesin complexes. Without STAG3, we see a general degeneration of meiotic progression, centromere cohesion, and homologous recombination, all features of the α-kleisins with which it is interacting. This idea has been previously supported in the field [59].

It is possible that α-kleisins are the main players in axis formation, and that the residual level of axis formation seen in the *Rad21l/Rec8* is due to the continued presence of RAD21 cohesins. It would be an interesting next step to determine if the amount of RAD21 expressed in the *Rad21l/Rec8* double mutant was higher or lower than in the wild type. An increase would suggest that there is a compensatory increase in RAD21, while a decrease would suggest that there is some sort of costimulatory/codependent interaction between the RAD21, RAD21L, and REC8 containing cohesin complexes. Another possibility arises with the NIPBL-MAU2 complex, implicated in the loading of cohesin onto chromatin in G1 [61-62]. Interaction with the cohesin ring is essential for this function, and its possible that

without RAD21L or REC8, two-thirds of the α-kleisins are gone, which may decrease the amount of NIPBL to facilitate the loading of cohesin. It is certainly important to note that our prior investigation into cohesins revealed that *Stag3* mutants saw an increase in the amount of RAD21 extracted from nuclei compared to wild type [6]. This may lend further support for the compensatory processes that may be taking place.

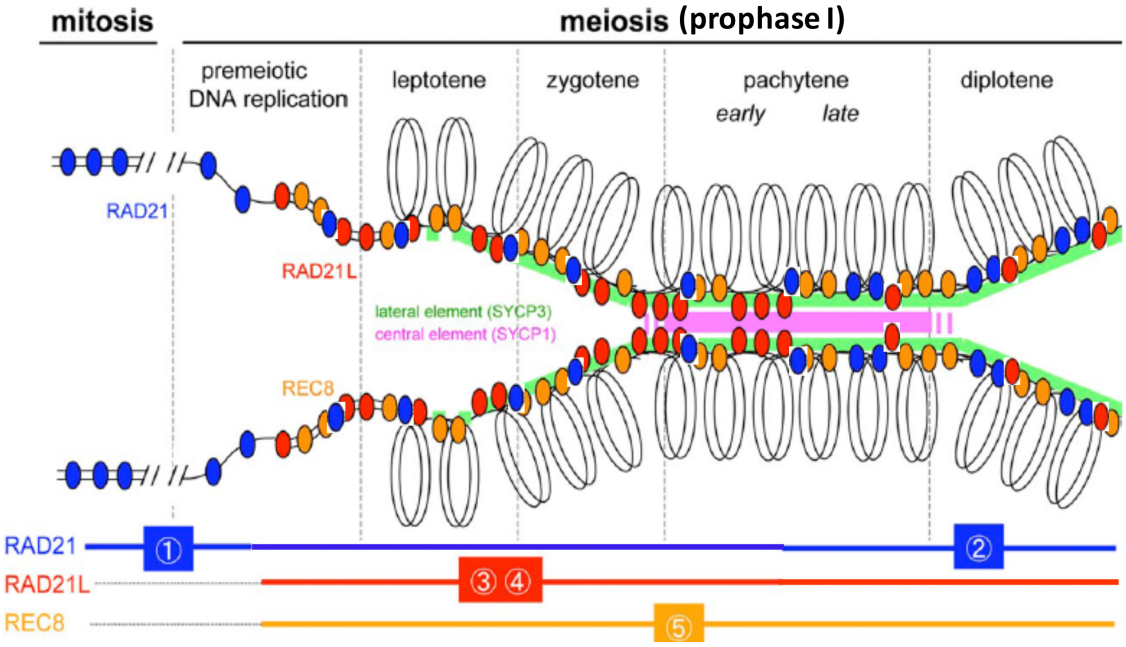

Figure 19: Model depicting the temporal separation of cohesin association to axes during prophase I. Figure modified from Lee and Hirano, 2011 [21].

STAG3 Requirement for Stability

Cohesin complexes have been shown to localize along the chromosomal axes during meiosis. It has been previously shown that there are up to 6 cohesin complexes active during meiosis, of which 5 are meiosis specific [10], [30], [33]. A solid body of work has elucidated the individual roles of the RAD21L, REC8, and RAD21 containing cohesins during this process [33], [35], [38]. Our lab has previously reported that the *Stag3* mutant exhibited reduction in colocalization of meiosis specific cohesin subunits, further lending itself to the idea that STAG3 is necessary for stability of the meiosis specific cohesin complex. To further investigate this role, we looked at the presence of cohesin components in our nuclear spreads. In the *Stag3/Rad21l* mutant, we observed a decrease in the available cohesin components (REC8, RAD21, SMC1B, SMC1A) (Fig.15-16). In the *Stag3/Rec8* mutants, we saw a similar decrease in meiosis specific subunits (RAD21L, RAD21, SMC1B, SMC1A) (Fig.15-16). Most remarkably, in the *Rad21l/Rec8* double mutant, we observed a decrease in all cohesin components (Fig.15-16). The fact that in spermatocytes mutated for two α-kleisin subunits we see a corresponding decrease in other α-kleisin proteins is striking.

These results give further evidence to our hypothesis that STAG3 is required for stabilization of the meiosis specific cohesin complex. Destabilization of the reciprocal α-kleisin subunit *in Stag3/Rad21l* and *Stag3/Rec8* mutants when no such reduction is observed in the *Rad21l* or *Rec8* mutants indicates that STAG3 may be responsible for the observed destabilization. Dependency of cohesin complexes upon STAG3 would suggest that STAG3's exclusivity in meiotic cohesin complex stabilization cannot be overridden.

Centromeres, Telomeres, and Pericentromeric Heterochromatin

The the early localization of the cohesin complex is important for sister chromatid cohesion, centromeric cohesion, and initiation of the dynamic movements that take place during prophase I via the telomere [30-31], [36-39], [56]. Meiosis specific cohesin components (STAG3, RAD21L, REC8) localize to the telomeres and chromocenters. Mouse chromosomes are telocentric, and this plays a role in prophase I. Telomeric attachments to the nuclear periphery to facilitate early chromosome pairing [7]. Cohesins containing STAG3 interact with telomeric protein TERB1, and stabilize the interaction between the telomere and the nuclear envelope [11], [58]. STAG3 is also important for maintaining centromeric cohesion [13] [55]. Defects in telomeric and centromeric cohesion lead to defects in meiotic progression, mainly in the ability to segregate chromosomes [63], [64]. Furthermore, the telocentric chromosome ends of mouse chromosomes contain large periheterochromatin domains, which tend to cluster (chromoclusters). These chromoclusters persist during meiosis to prevent aberrant recombination events that can lead to segregation and progression errors in meiosis. Cohesin localization to these areas only further implicates it in maintaining the stability of chromosome movements, as evidenced by the necessity of REC8 localization to these areas [45]. Thus the case can be made for an interdependency between the chromocenters, centromeres, and telomeres in early prophase chromosome dynamics.

In the *Rec8* and *Stag3* mutants, we saw a marked decrease in centromere cohesion, and an increase in the number of chromoclusters, suggesting a decrease in clustering (Fig.14, Fig.18). This is consistent with the reported functions of STAG3 in cohesin stability, and REC8 in centromere cohesion at chromosome ends [6], [37], [54], [59]. In the *Rad21l* mutant, we did not see a comparable decrease in centromere cohesion to the *Stag3* or *Rec8* mutants, consistent with the observation that RAD21L is not required for proper centromeric cohesion during meiosis [36]. This same mutant showed an overall lower number of

chromocenters, which were visibly larger in size than those of the wild type, *Rec8*, or *Stag3* mutants (Fig.18A). RAD21L may not be implicated in centromeric cohesion, but one of its known functions involves proper synapsis between homologues. The fact that we see a decrease in the number of chromocenters may allude to why we see non-homologous interactions without RAD21L. Part of the initial homology search is initiated by the accumulation of chromocenters, and RAD21L localizes to these regions, therefore, it is possible that errant chromocenters are the reason that we see non-homologous recombination in these mutants. In the *Stag3/Rad21l* and *Stag3/Rec8* mutants, we saw a substantial decrease in centromere cohesion, which is logical given the individual phenotypes of *Stag3/Rad21l,* and *Rec8* mutants (Fig.14). However, in the *Stag3/Rad21l* mutant we see what appears to be an intermediate between the *Rad21l* mutant and the *Stag3* mutant. This can be explained by the fact that the *Stag3* mutant also affects the stability of the REC8 cohesin complex, and in-turn disrupts centromeric cohesion between sister chromatids, and thus increases pericentromeric heterochromatin cluster numbers.

In the *Rad21l/Rec8* double mutant, we saw a distinct reduction of centromere number consistent with the fact that chromosomal axes are greatly perturbed (Fig.14). The reduction in centromere number could be explained by overlap of their signal making them indistinguishable from one another. This result was further corroborated by the presence of an average of 3 large chromocenters (Fig.18), indicating that the presence of the *Rad21l* mutation was having a similar effect when combined with *Rec8* mutation. Taken together, the phenotypes described for the *Rad21l/Rec8* double mutant argues that STAG3 is required for stability of cohesin complexes on chromosomes, rather than their initial loading. The *Rad21l/Rec8* double mutant displays a leptotene-like arrest, whereas the *Stag3* mutant, together with the *Stag3/Rad21l* and *Stag3/Rec8* double mutants arrest at a zygotene-like stage.

Possible role for mitotic cohesins in meiosis

In our chromatin spreads, the level of the mitotic α-kleisin, RAD21, was relatively undisturbed. This is the expected result since we are not perturbing its gene. However, it raises some questions. While we do see a marked decrease in stability of axis formation in cohesin mutants, we still see a chromosome axis formation independent of STAG3. If STAG3 really is the exclusive STAG protein present in meiotic cohesin complexes, it would follow that we should not see any axis formation in these chromatin spreads. Our observations to the contrary suggest that there is a mechanism or protein interaction in place that is preventing complete axial destabilization, although its nature is not yet known. Given the sequence homology between STAG 1, 2, and 3 α-kleisin interaction domains, and the apparent stability of the RAD21 containing cohesins, we thought it was possible that mitotic STAG proteins STAG1 or STAG2 may be compensating for the lack of STAG3 in these mutants, forming a complete cohesin complex. Conflicting observations have been made in the past on both the ability of STAG1/2 to interact with meiosis specific cohesin components in *Stag3* mutants. Some studies indicate the ability of STAG1/2 to co-precipitate with SMC1B, while others show the opposite [13], [30], [59]. In our chromatin spreads of *Stag3* mutants we did not see any notable localization of STAG1 or 2 to chromosomal axes, corroborating earlier observations of its absence (Supplementary Fig.S4).

This result presents several possibilities. Based on observations made in previous studies, it is possible that the level of STAG1/2 is adequate for detection via immunoprecipitation, but below the level of detection via immunofluorescence microscopy. However, this would not explain the conflicting evidence of SMC1B interactions [30], [59].

Finally, with the continued localization of RAD21 on chromosomal axes, it may be that a STAG protein is not required for the cohesin complex to localize to axes. This would concur with the data suggesting that we still see chromosomal axes forming in STAG3 deficient prophase spermatocytes. In addition, our data supports our hypothesis that STAG3 is necessary for the stability of the cohesin complexes at the chromosome axes, and not their initial localization to the axes. These results should also be considered with the *Rad21l/Rec8* double mutant, which clearly shows RAD21 cohesins localizing to chromosomal axes, although these axes are short and few in number (Fig.13A). It is possible that the α-kleisins RAD21, RAD21L, and REC8 form a tripartite cohesin balance during meiosis. All three contributing to chromosome axis formation. Knocking out two-thirds of that balance severely cripples axis formation, but does not destroy it completely. It would be interesting to see whether there is axis formation in a *Rad21l/Rec8* mutant treated with siRNA against RAD21 or use of a conditional mutant for *Rad21*.Alternatively, we could test whether overexpression of separase within prophase I meiocytes of a *Stag3* mutant (given STAG3's protective function of the α-kleisin would affect axis formation).

PUBLIC HEALTH RELEVANCE

Our data on STAG3 have indicated that it is necessary for the adequate progression of meiosis. Although we use the mouse as a model, STAG3 research has direct relevance on human diseases, and issues of public health. *Stag3* mutation has recently been implicated as a defect in male and female infertility [60], [65-66]. Other studies have linked both STAG3 and the cohesin complex itself in non-fertility related diseases. Cohesin complex proteins, have been continuously found to be mutated or incorrectly expressed in pre-leukemic hematopoietic stem and progenitor cells [65]. Thus, it is theorized that these mutations are key initiating steps in the pathogenesis of acute myeloid leukemia (AML). Furthermore, we see Human Papillomavirus, for example, has been shown to activate and recruit SMC1 cohesin proteins to aid in genome amplification and propagation [66]. Another disease that implicates cohesin dysfunction is colorectal cancer. It has been shown that there is a correlation between errant expression of RAD21 in males and shorter survival for colorectal carcinomas [67]. Finally, Cornelia de Lange syndrome is a multiple malformation disorder characterized by dysmorphic facial features, mental retardation, growth delay, and limb reduction defects. Recent studies into this disease have implicated cohesin component mutations in the pathogenesis of the disease (RAD21, SMC1α, and SMC3) [69-71]. Given that the cohesin complex's full interacting partners, and even its form in the nucleus are under debate, it is likely that continued study of this impressive protein complex will lead to advances in our understanding of these diseases and more.

CONCLUSION

Using three independent null mutations for *Rad21l*/*Rec8*, and *Stag3*. as well as three novel null mutations for the *Stag3*/*Rad21l*, *Stag3*/*Rec8*, and *Rad21l*/*Rec8* genotypes, we have given further indication towards the necessity of STAG3 for the stability of the cohesin complex in meiosis. We show that the *Stag3*/*Rad21l* and*Stag3*/*Rec8* double mutant mice to exhibit more pronounced meiotic defects than the single mutants, namely an increased number of unsynapsed axes, shortening of axes, and centromere cohesion defects. Furthermore, we show that while these phenotypes are more severe than the *Stag3* mutant, they are not as severe as the *Rad21l*/*Rec8* double mutant, which lacks axis formation, and displays little to no cohesin localization. These proposed observations support our hypothesis that STAG3 is required for the stability of meiosis-specific cohesins, but not the ability to associate with the chromosome axes during meiosis.

APPENDIX

S1: Analysis of Stag3 JAX Litter SYCP3 Axes

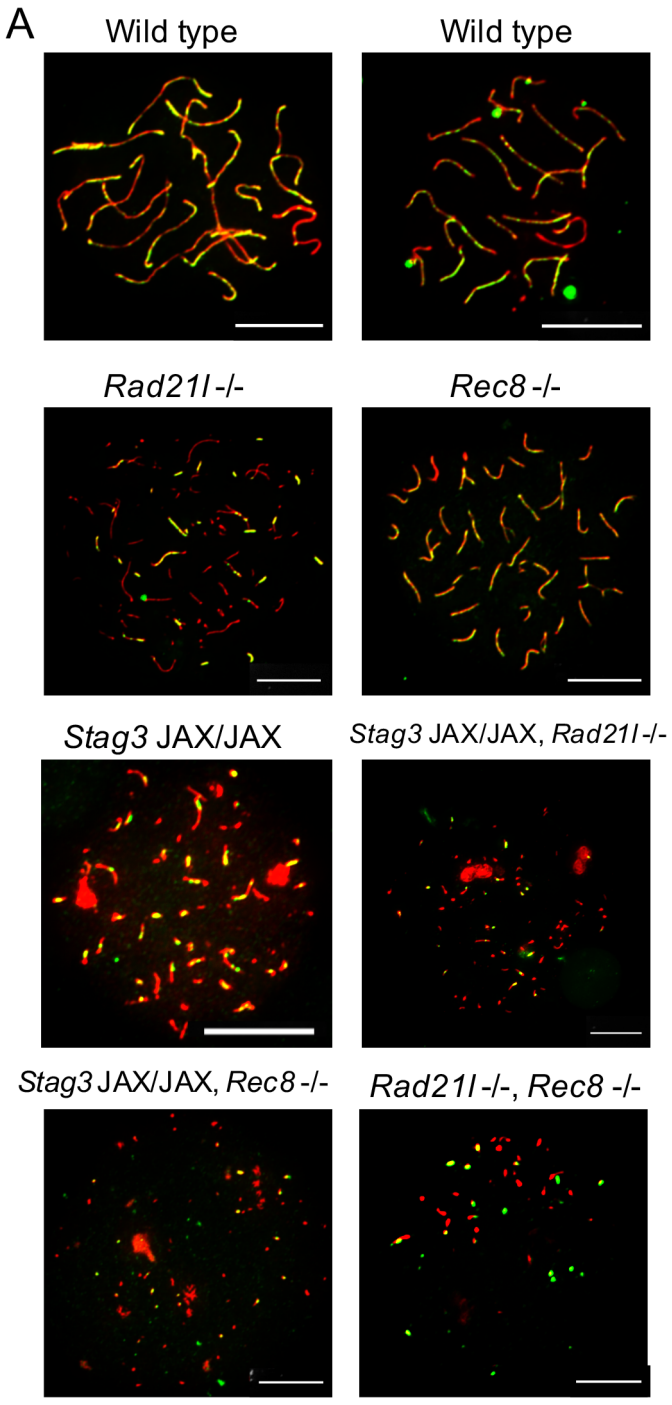

Figure S1: Microscopy and Analysis of SYCP3 localization in meiotic prophase I of *Stag3 JAX* allele mice. (A) Microscopy of DPP=15 mouse chromatin spreads acquired from the testis. Images show SYCP3 (Red) localization to the chromosome axes, and colocalization of SYCP1 (green) to these same axes as a mark of progression through prophase. Areas of colocalization appear yellow in color (n=25). All scale bars set to 10 μm.

S1: Analysis of Stag3 JAX Litter SYCP3 Axes (cont.)

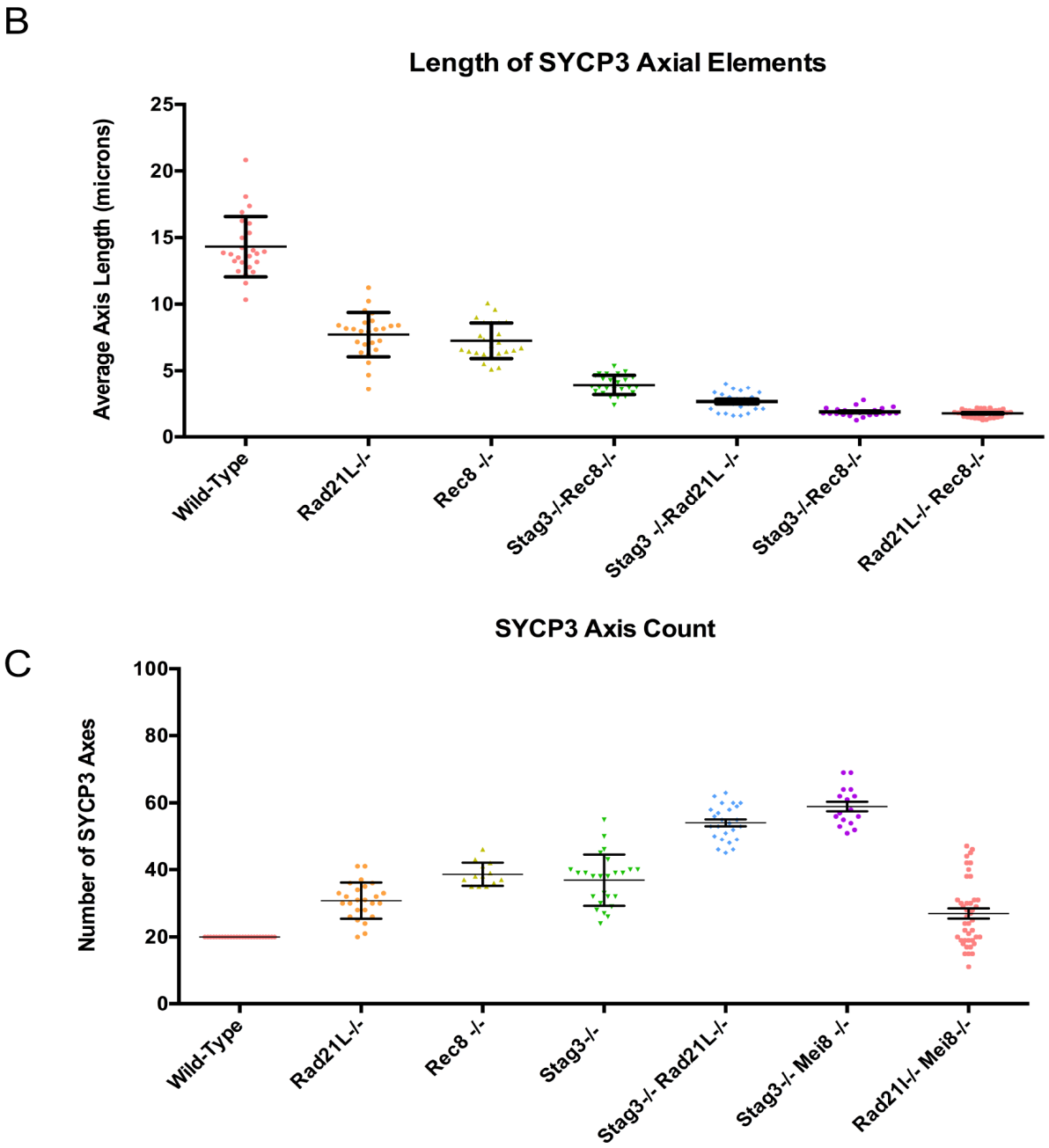

Figure S1: Microscopy and Analysis of SYCP3 localization in meiotic prophase I of *Stag3 JAX* allele mice. (B) Analysis of axis length in chromatin spreads during meiotic prophase I (n=25). (C) Analysis of the number of SYCP3 stained axes present in meiotic prophase I. The X axis shows the genotype in (B) and (C) (n=25).

S2: Analysis of Stag3 JAX Litter Centromere Localization

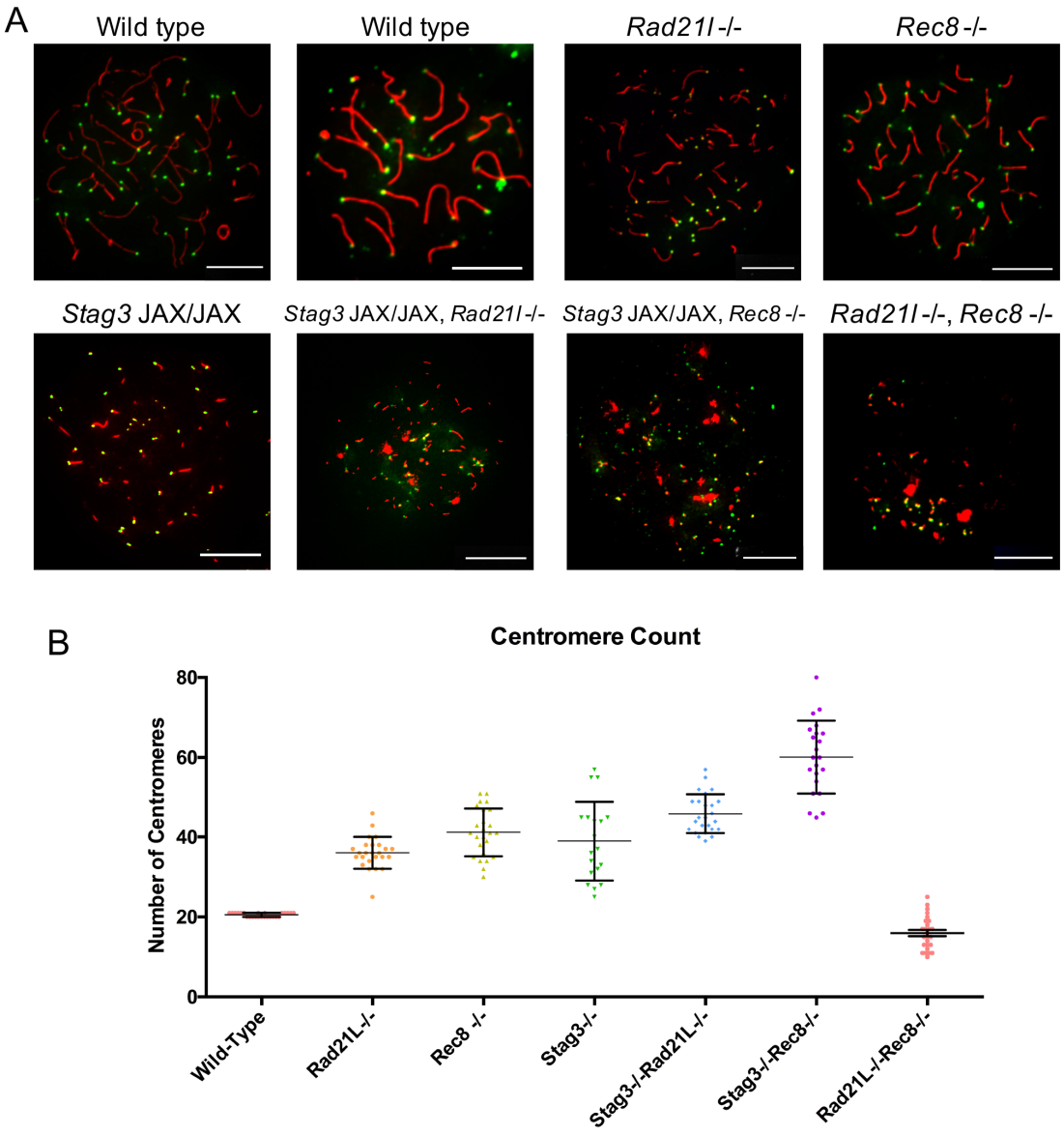

Figure S2: Centromere Microscopy. (A) Images showing colocalization of SYCP3 (red) and Centromere (green). (B) Quantification of the average number of centromere signals counted in each individual spread (n=50). The Y axis depicts the genotype of the spreads in question. All scale bars set to 10 μm.

S3: Analysis of H2AX Signal in Cohesin Deficient Spermatocytes

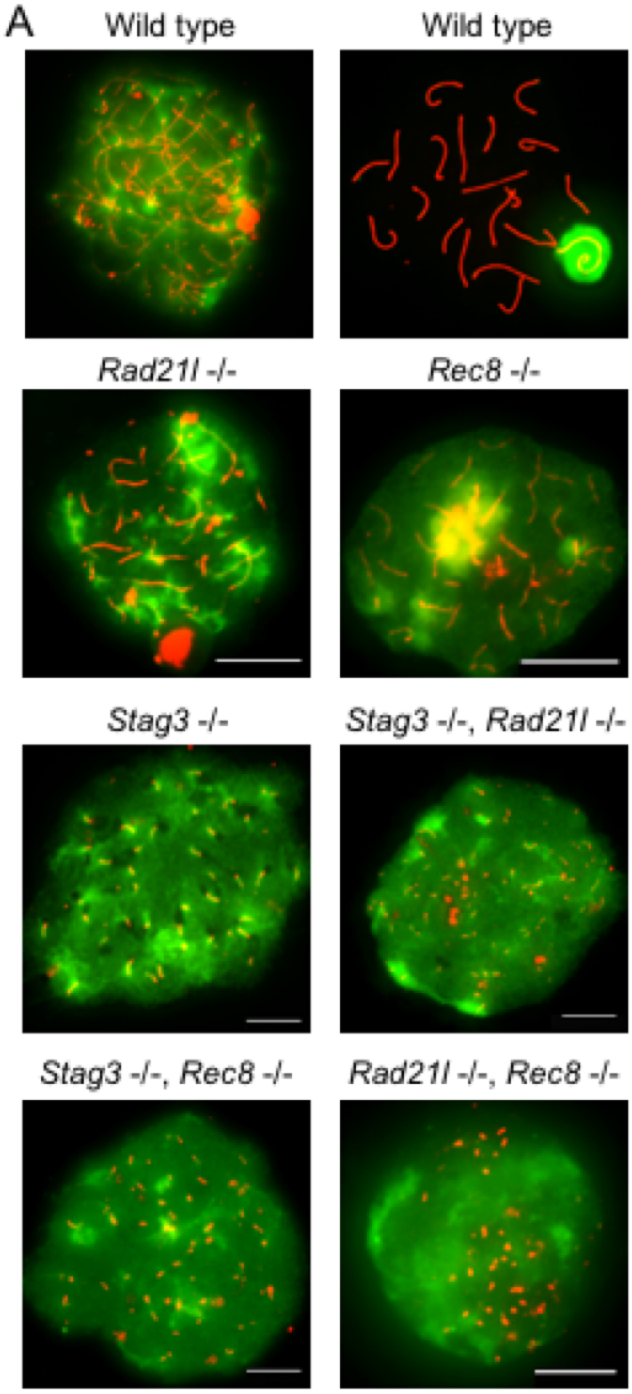

Figure S4: Immunofluroesence microscopy visualizing the presence of DNA damage signal γH2AX (green) in nuclear spreads stained for SYCP3 (red). All scale bars set to 10 μm.

S4: Analysis of STAG 1 and 2 Presence in STAG3 OV Mutations

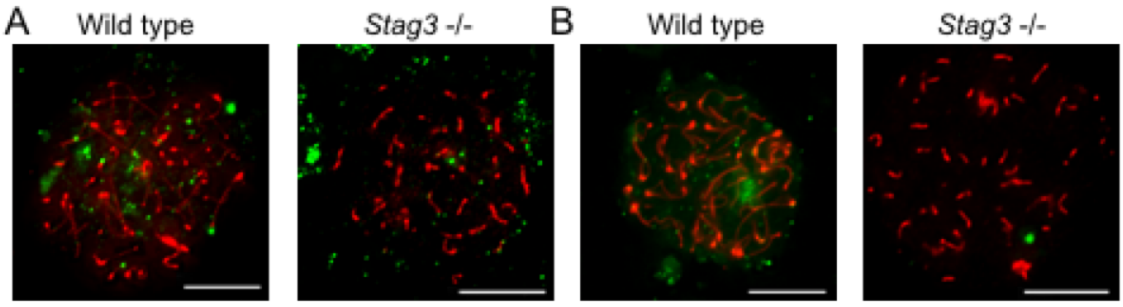

Figure S4: Immunofluroesence microscopy visualizing the presence of DNA damage signal γH2AX (green) in nuclear spreads stained for SYCP3 (red). All scale bars set to 10 μm.

REFERENCES

1. Tropp, Burton E., and David Freifelder. "Chapter 6: Chromosome Structure." Molecular Biology: Genes to Proteins. Sudbury, MA: Jones and Bartlett, 2008. 180-81. Print.
2. Subramanian, Vijayalakshmi V., and Andreas Hochwagen. "The meiotic checkpoint network: step-by-step through meiotic prophase." *Cold Spring Harbor perspectives in biology* 6.10 (2014): a016675.
3. Jordan, P. "Initiation of homologous chromosome pairing during meiosis." *Biochemical Society Transactions* 34.4 (2006): 545-549.
4. Bisig, C. Gaston, et al. "Synaptonemal complex components persist at centromeres and are required for homologous centromere pairing in mouse spermatocytes." *PLoS genetics* 8.6 (2012): e1002701.
5. Qiao, Huanyu, et al. "Interplay between synaptonemal complex, homologous recombination, and centromeres during mammalian meiosis." *PLoS genetics* 8.6 (2012): e1002790.
6. Hopkins, Jessica, et al. "Meiosis-specific cohesin component, Stag3 is essential for maintaining centromere chromatid cohesion, and required for DNA repair and synapsis between homologous chromosomes." *PLoS genetics* 10.7 (2014): e1004413.
7. Scherthan, Harry, et al. "Centromere and telomere movements during early meiotic prophase of mouse and man are associated with the onset of chromosome pairing." *The Journal of Cell Biology* 134.5 (1996): 1109-1125
8. Levan, Albert, Karl Fredga, and Avery A. Sandberg. "Nomenclature for centromeric position on chromosomes." *Hereditas* 52.2 (1964): 201-220.

9. Parra, María Teresa, et al. "Sequential assembly of centromeric proteins in male mouse meiosis." *PLoS Genet* 5.3 (2009): e1000417-e1000417
10. Ishiguro, Kei-ichiro, et al. "A new meiosis-specific cohesin complex implicated in the cohesin code for homologous pairing." *EMBO reports* 12.3 (2011): 267-275
11. Hiraoka, Yasushi, and Abby F. Dernburg. "The SUN rises on meiotic chromosome dynamics." *Developmental cell* 17.5 (2009): 598-605.
12. Skarnes, William C., et al. "A conditional knockout resource for the genome-wide study of mouse gene function." *Nature* 474.7351 (2011): 337-342
13. Fukuda, Tomoyuki, et al. "STAG3-mediated stabilization of REC8 cohesin complexes promotes chromosome synapsis during meiosis." *The EMBO journal* (2014): e201387329
14. McKee, Bruce D., and Mary Ann Handel. "Sex chromosomes, recombination, and chromatin conformation." *Chromosoma* 102.2 (1993): 71-80.
15. Baudat, Frédéric, et al. "Chromosome synapsis defects and sexually dimorphic meiotic progression in mice lacking Spo11." *Molecular cell* 6.5 (2000): 989-998.
16. Prieler, Silvia, et al. "The control of Spo11's interaction with meiotic recombination hotspots." *Genes & development* 19.2 (2005): 255-269.
17. Longhese, Maria Pia, et al. "DNA double-strand breaks in meiosis: checking their formation, processing and repair." *DNA repair* 8.9 (2009): 1127-1138.
18. Royo, Hélène, et al. "ATR acts stage specifically to regulate multiple aspects of mammalian meiotic silencing." *Genes & development* 27.13 (2013): 1484-1494.

19. de Vries, Femke AT, et al. "Mouse Sycp1 functions in synaptonemal complex assembly, meiotic recombination, and XY body formation." *Genes & development* 19.11 (2005): 1376-1389.
20. Fraune, Johanna, et al. "The mammalian synaptonemal complex: protein components, assembly and role in meiotic recombination." *Experimental cell research* 318.12 (2012): 1340-1346.
21. Sun, Fengyun, and Mary Ann Handel. "Regulation of the meiotic prophase I to metaphase I transition in mouse spermatocytes." *Chromosoma* 117.5 (2008): 471-485.
22. Marini, Victoria, and Lumir Krejci. "Unwinding of synthetic replication and recombination substrates by Srs2." *DNA repair* 11.10 (2012): 789-798.
23. Moldovan, George-Lucian, et al. "Inhibition of homologous recombination by the PCNA-interacting protein PARI." *Molecular cell* 45.1 (2012): 75-86.
24. Bugreev, Dmitry V., et al. "Novel pro-and anti-recombination activities of the Bloom's syndrome helicase." *Genes & development* 21.23 (2007): 3085-3094.
25. Hu, Yiduo, et al. "RECQL5/Recql5 helicase regulates homologous recombination and suppresses tumor formation via disruption of Rad51 presynaptic filaments." *Genes & development* 21.23 (2007): 3073-3084.
26. Sommers, Joshua A., et al. "FANCJ uses its motor ATPase to destabilize protein-DNA complexes, unwind triplexes, and inhibit RAD51 strand exchange." *Journal of Biological Chemistry* 284.12 (2009): 7505-7517.

27. Bolcun-Filas, Ewelina, et al. "Mutation of the mouse Syce1 gene disrupts synapsis and suggests a link between synaptonemal complex structural components and DNA repair." *PLoS genetics* 5.2 (2009): e1000393.
28. Tarsounas, Madalena, et al. "RAD51 and DMC1 form mixed complexes associated with mouse meiotic chromosome cores and synaptonemal complexes." *The Journal of cell biology* 147.2 (1999): 207-220.
29. Verver, Dideke E., et al. "Resolving complex chromosome structures during meiosis: versatile deployment of Smc5/6." *Chromosoma* (2015): 1-13.
30. Lee, Jibak, and Tatsuya Hirano. "RAD21L, a novel cohesin subunit implicated in linking homologous chromosomes in mammalian meiosis." *The Journal of cell biology* 192.2 (2011): 263-276.
31. Losada, Ana, and Tatsuya Hirano. "Dynamic molecular linkers of the genome: the first decade of SMC proteins." *Genes & development* 19.11 (2005): 1269-1287.
32. Strunnikov, Alexander V., and Rolf Jessberger. "Structural maintenance of chromosomes (SMC) proteins." *European Journal of Biochemistry* 263.1 (1999): 6-13.
33. Gutiérrez-Caballero, Cristina, et al. "Identification and molecular characterization of the mammalian α-kleisin RAD21L." *Cell Cycle* 10.9 (2011): 1477-1487.
34. Watanabe, Yoshinori, and Paul Nurse. "Cohesin Rec8 is required for reductional chromosome segregation at meiosis." *Nature* 400.6743 (1999): 461-464
35. Xu, Huiling, et al. "A new role for the mitotic RAD21/SCC1 cohesin in meiotic chromosome cohesion and segregation in the mouse." *EMBO reports* 5.4 (2004): 378-384

36. Herrán, Yurema, et al. "The cohesin subunit RAD21L functions in meiotic synapsis and exhibits sexual dimorphism in fertility." *The EMBO Journal* 30.15 (2011): 3091-3105.

37. Bannister, Laura A., et al. "Positional cloning and characterization of mouse mei8, a disrupted allele of the meiotic cohesin Rec8." *Genesis* 40.3 (2004): 184-194.

38. Adelfalk, Caroline, et al. "Cohesin SMC1β protects telomeres in meiocytes." *The Journal of cell biology* 187.2 (2009): 185-199.

39. Xu, Huiling, et al. "Rad21-cohesin haploinsufficiency impedes DNA repair and enhances gastrointestinal radiosensitivity in mice." *PLoS One* 5.8 (2010): e12112.

40. Urban, Evelin, et al. "The cohesin subunit Rad21 is required for synaptonemal complex maintenance, but not sister chromatid cohesion, during Drosophila female meiosis." (2014): e1004540.

41. Pezzi N, Prieto I, Kremer L, Perez Jurado LA, Valero C, Del Mazo J, Martinez AC, Barbero JL (2000) STAG3, a novel gene encoding a protein involved in meiotic chromosome pairing and location of STAG3-related genes flanking the Williams-Beuren syndrome deletion. *FASEB J* **14**: 581–592

42. Canudas S, Smith S (2009) Differential regulation of telomere and centromere cohesion by the Scc3 homologues SA1 and SA2, respectively, in human cells. *J Cell Biol* **187**: 165–173

43. Hauf S, Roitinger E, Koch B, Dittrich CM, Mechtler K, Peters JM (2005) Dissociation of cohesin from chromosome arms and loss of arm cohesion during early mitosis depends on phosphorylation of SA2. *PLoS Biol* **3**: e69

44. Prieto I, Pezzi N, Buesa JM, Kremer L, Barthelemy I, Carreiro C, Roncal F, Martinez A, Gomez L, Fernandez R, Martinez AC, Barbero JL (2002) STAG2 and Rad21 mammalian mitotic cohesins are implicated in meiosis. *EMBO Rep* **3**: 543–55

45. Kitajima, Tomoya S., et al. "Shugoshin collaborates with protein phosphatase 2A to protect cohesin." *Nature* 441.7089 (2006): 46-52.

46. Riedel, Christian G., et al. "Protein phosphatase 2A protects centromeric sister chromatid cohesion during meiosis I." *Nature* 441.7089 (2006): 53-61.

47. Clift, D., and A. L. Marston. "The role of shugoshin in meiotic chromosome segregation." *Cytogenetic and genome research* 133.2-4 (2011): 234-242.

48. Kitajima, Tomoya S., et al. "Rec8 cleavage by separase is required for meiotic nuclear divisions in fission yeast." *The EMBO journal* 22.20 (2003): 5643-5653.

49. Giménez-Abián, Juan F., et al. "Regulation of sister chromatid cohesion between chromosome arms." *Current biology* 14.13 (2004): 1187-1193.

50. Sumara, Izabela, et al. "The dissociation of cohesin from chromosomes in prophase is regulated by Polo-like kinase." *Molecular cell* 9.3 (2002): 515-525.

51. Zhang, Nenggang, and Debananda Pati. "Handcuff for sisters: a new model for sister chromatid cohesion." *Cell Cycle* 8.3 (2009): 399-402

52. Llano, Elena, et al. "Meiotic cohesin complexes are essential for the formation of the axial element in mice." *The Journal of cell biology* 197.7 (2012): 877-885.

53. Skarnes, William C., et al. "A conditional knockout resource for the genome-wide study of mouse gene function." *Nature* 474.7351 (2011): 337-342.

54. Xu, Huiling, et al. "Absence of mouse REC8 cohesin promotes synapsis of sister chromatids in meiosis." *Developmental cell* 8.6 (2005): 949-961.

55. Bisig, C. Gaston, et al. "Synaptonemal complex components persist at centromeres and are required for homologous centromere pairing in mouse spermatocytes." *PLoS genetics* 8.6 (2012): e1002701.

56. Buonomo, Sara BC, et al. "Disjunction of homologous chromosomes in meiosis I depends on proteolytic cleavage of the meiotic cohesin Rec8 by separin." *Cell* 103.3 (2000): 387-398.

57. Scherthan, Harry, et al. "Centromere and telomere movements during early meiotic prophase of mouse and man are associated with the onset of chromosome pairing." *The Journal of Cell Biology* 134.5 (1996): 1109-1125

58. Shibuya, Hiroki, Kei-ichiro Ishiguro, and Yoshinori Watanabe. "The TRF1-binding protein TERB1 promotes chromosome movement and telomere rigidity in meiosis." *Nature cell biology* 16.2 (2014): 145-156.

59. Winters, Tristan, Francois McNicoll, and Rolf Jessberger. "Meiotic cohesin STAG3 is required for chromosome axis formation and sister chromatid cohesion." *The EMBO journal* (2014): e201387330.

60. Llano, Elena, et al. "STAG3 is a strong candidate gene for male infertility." *Human molecular genetics* 23.13 (2014): 3421-3431.

61. Kuleszewicz, Katarzyna, Xiangwei Fu, and Nobuaki R. Kudo. "Cohesin loading factor Nipbl localizes to chromosome axes during mammalian meiotic prophase." *Cell division* 8.1 (2013): 12.

62. Dorsett, Dale. "Cohesin: genomic insights into controlling gene transcription and development." *Current opinion in genetics & development* 21.2 (2011): 199-206.

63. Zhang, Nenggang, et al. "A handcuff model for the cohesin complex." *The Journal of cell biology* 183.6 (2008): 1019-1031.

64. Liu, Lin, et al. "Irregular telomeres impair meiotic synapsis and recombination in mice." *Proceedings of the National Academy of Sciences of the United States of America* 101.17 (2004): 6496-6501

65. Nelson, Lawrence M. "Primary ovarian insufficiency." *New England Journal of Medicine* 360.6 (2009): 606-614.

66. Matzuk, Martin M., and Dolores J. Lamb. "The biology of infertility: research advances and clinical challenges." *Nature medicine* 14.11 (2008): 1197-1213.

67. Mazumdar, Claire, et al. "Cohesin Complex Mutations Impair Differentiation of Human Hematopoietic Stem and Progenitor Cells." *Blood* 124.21 (2014): 4785-4785.

68. Mehta, Kavi, et al. "Human Papillomaviruses Activate and Recruit SMC1 Cohesin Proteins for the Differentiation-Dependent Life Cycle through Association with CTCF Insulators." (2015): e1004763.

69. Deardorff, Matthew A., et al. "Mutations in cohesin complex members SMC3 and SMC1A cause a mild variant of Cornelia de Lange syndrome with predominant mental retardation." *The American Journal of Human Genetics* 80.3 (2007): 485-494.

70. Deardorff, Matthew A., et al. "HDAC8 mutations in Cornelia de Lange syndrome affect the cohesin acetylation cycle." *Nature* 489.7415 (2012): 313-317.

71. Kline, Antonie D., et al. "Cornelia de Lange syndrome: Further delineation of phenotype, cohesin biology and educational focus, 5th Biennial Scientific and Educational Symposium abstracts." *American Journal of Medical Genetics Part A* 164.6 (2014): 1384-1393.

CURRICULUM VITAE

Ayobami L. Ward

(509) 591-8574 | a.ward3@me.com
2807 Cresmont Avenue | Apt 604D | Baltimore, MD 21211

EDUCATION

Johns Hopkins Bloomberg School of Public Health – Baltimore, MD 2015
Master of Science: Biochemistry & Molecular Biology, Certificate: Vaccine Science and Application
Krieger School of Arts and Sciences, Johns Hopkins University – Baltimore, MD 2013
Bachelor of Science: Neuroscience, Minor: Entrepreneurship and Management

---

EXPERIENCE

Johns Hopkins Bloomberg School of Public Health - Baltimore, MD 2014 – 2015
Research Assistant; Dr. Phil Jordan, Ph.D.

- Designing experiments to evaluate phenotype of novel conditional-KO mice for meiosis specific cohesion proteins collected from testis/ovaries.
- Extracting, amplifying, and quantifying data from DNA and RNA for use in PCR and confocal/deconvolution immunofluorescence microscopy.
- General lab maintenance including solution preparation, and ordering. .

Johns Hopkins University, Nu Rho Psi Undergraduate Honors Society – Baltimore, MD 2011 - 2014
Vice President of Volunteering, Teacher for Making Neuroscience Fun (MNF)

Johns Hopkins University, Department of Psychological and Brain Science - Baltimore, MD 2012 – 2014
Research Assistant; Dr. Michael Yassa, Ph.D.

- Collaborated with Ph.D. candidates and two undergraduate students to elucidate a cure for Alzheimer's
- Programmed and debugged three core simulations to test pattern recognition and memory inn MatLab
- Utilized fMRI-scanning centers to monitor brain activity in real time to complement numerical data results
- Developed two experiments to investigate the effects of hormonal imbalances on female depression
- HPLC to test salivary fluids for presence of enzymes implicated in digestion of caffeine.

Johns Hopkins Medical Institute, Department of Neurosurgery 2011 – 2013
Clinical Research Assistant: Dr. Daniele Rigamonti

Publications

- Moran, Dane, et al. "Does CT wand guidance improve shunt placement in patients with Hydrocephalus?" *Clinical Neurology and Neurosurgery* (2015).
- Goodwin, C. Rory, et al. "Risk factors for failed transverse sinus stenting in pseudotumor cerebri patients." *Clinical neurology and neurosurgery* 127 (2014): 75-78.
